Short title: *Medicago*'s responses to variable benefit AM fungi

Author for Contact details: Heike Bücking, South Dakota State University, Biology and Microbiology Department, Brookings, SD 57007, USA

Physiological and transcriptomic response of *Medicago truncatula* to high and low benefit mycorrhizal fungi

Kevin R. Cope[1†], Arjun Kafle[1,2,†], Jaya K. Yakha[1], Philip E. Pfeffer[3], Gary D. Strahan[3], Kevin Garcia[2], Senthil Subramanian[1,4], Heike Bücking[1]

[1]South Dakota State University, Biology and Microbiology Department, Brookings, SD 57007, USA;

[2]Department of Crop and Soil Sciences, North Carolina State University, Raleigh, NC 27695-7619, USA;

[3]USDA, Agricultural Research Service, Eastern Regional Research Center, 600 East Mermaid Lane, Wyndmoor, PA, 19038, USA;

[4]Department of Agronomy, Horticulture, and Plant Science, South Dakota State University, Brookings, SD, 57007, USA.

[†]These Authors contributed equally to the work.

One sentence summary: Colonization with high- and low-benefit arbuscular mycorrhizal fungi leads to distinct physiological and transcriptomic changes in the roots and shoots of *Medicago truncatula*.

Footnotes:

List of Author contributions. H.B. and S.S. conceived the original research plans; H.B. and A.K. designed the experiments; A.K. performed the long-term experiment and J.Y. the short-term experiment, K.R.C. and K.G. conducted the transcriptome analysis, and P.P. and G.S. completed the stable isotope analysis; K.R.C., A.K., K.G., J.Y. and P.P. analyzed the data; K.R.C. wrote the article with input from all the authors; H.B. and S.S. supervised and completed the writing. H.B. agrees to serve as the author responsible for contact and ensures communication.

Responsibilities of the Author for Contact. The corresponding author, Heike Bücking, ensures that all scientists who have contributed substantially to the conception, design, or execution of the work are included as authors, and that all authors have agreed to the list of authors and to the identified contributions of the authors.

Funding information. This work was funded by the USDA (2017-67014-26530), the SD Soybean Research and Promotion Council, and the Agricultural Experiment Station at SDSU to HK and SS. KG acknowledges support of the North Carolina Agriculture Research Service (NCARS), the North Carolina Soybean Producers Association (2019-1656), and the USDA (2020-67013-31800).

Email address of Author for Contact: Heike Bücking, Email: heike.bucking@sdstate.edu

ABSTRACT

Arbuscular mycorrhizal (AM) fungi provide their host plants with greater access to limited mineral nutrients, but the amount they provide can be variable. Here, we evaluated the capacity of the high-benefit fungus *Rhizophagus irregularis* 09 and the low-benefit fungus *Glomus aggregatum* 165 to transfer nitrogen and phosphorus to the host plant *Medicago truncatula*, and identified putative molecular mechanisms regulating the physiological response of the host to these fungi. *R. irregularis* led to an increase in plant biomass and transferred more nitrogen and phosphate to the host than *G. aggregatum*. This increase was linked to elevated expression of known mycorrhiza-induced phosphate (*PT8*), ammonium (*AMT2;3*), and nitrate (*NPF4.12*) transporters in the roots, as well as the putative ammonium transporter *NIP1;5*. *R. irregularis* also stimulated the expression of photosynthesis related genes in the shoot and the upregulation of the mycorrhiza-induced sugar transporter *SWEET1.2* and the lipid biosynthesis gene *RAM2* in the roots, which is indicative of increased carbon flux to this fungus. In contrast, *G. aggregatum* induced biotic stress defense response genes (e.g., *Medtr4g120760* and *Medtr8g096900*) in the shoots, and several genes associated with the GO term "response to water deprivation" in the roots of *M. truncatula.* This could indicate that the host perceives colonization by the low-benefit fungus as pathogen attack, or that *G. aggregatum* is more effective than *R. irregularis* at priming host defense responses. Our findings reveal novel insights into the molecular mechanisms by which host plants reward high- but sanction low-benefit arbuscular mycorrhizal symbionts.

67 **INTRODUCTION**

68 Nitrogen (N) and phosphorus (P) are the main nutrients that limit plant growth in natural and
69 agricultural ecosystems (LeBauer and Treseder, 2008; Vitousek et al., 2010). Conventional
70 management practices typically address both N and P limitations through the application of
71 chemical fertilizers, but fertilizer production, transportation, and application are both economically
72 and environmentally expensive (Havlin et al., 2014). Implementing more sustainable methods to
73 mitigate nutrient deficiencies in crops is essential to prevent continued environmental degradation
74 but still meet the nutritional demands of a growing human population.

75 To overcome nutrient limitations, plants have evolved the capacity to form alliances with
76 symbiotic, root-associated microbes (Martin et al., 2017). The most widespread symbiosis is the
77 arbuscular mycorrhizal (AM) symbiosis formed by 72% of all known plant species and a relatively
78 small number of fungal species in the Glomeromycotina (Spatafora et al., 2016; Brundrett and
79 Tedersoo, 2018). AM fungi provide the host plant with mineral nutrients, such as P and N, and
80 improve the resistance of plants against abiotic and biotic stresses (Bücking and Kafle, 2015; Kafle
81 et al., 2019). Under P deficiency, plants increase the production of strigolactones, a class of
82 phytohormones that also serve as signaling molecules perceived by AM fungi (Yoneyama et al.,
83 2007). Strigolactones are exuded into the rhizosphere through the ATP-binding cassette transporter
84 PDR1 (Kretzschmar et al., 2012). AM fungal perception of strigolactones triggers spore
85 germination, hyphal branching, and the production of short-chain chitin oligomers (Besserer et al.,
86 2008; Genre et al., 2013). These, along with lipo-chitooligosaccharides (Maillet et al., 2011; Rush
87 et al., 2020), comprise fungal "Myc factors" that prime the host plant for colonization by activating
88 the "common symbiosis signaling pathway" (CSSP; reviewed in MacLean et al., 2017).

89 Activation of the CSSP by AM fungi culminates in the expression of several transcription
90 factors required for the development and regulation of the AM symbiosis (Pimprikar and Gutjahr,
91 2018). Following root penetration, AM hyphae proliferate both intra- and intercellularly and form
92 highly branched nutrient exchange structures called arbuscules in cortical cells (Park et al., 2015).
93 Surrounding the arbuscule is a plant-derived periarbuscular membrane (PAM) that is enriched in
94 AM-induced transporters that facilitate reciprocal nutrient exchange between the fungus and the
95 plant (Garcia et al., 2016). In *Medicago truncatula*, three AMT2 family ammonium transporters
96 (AMT2;3, AMT2;4, and AMT2;5; Breuillin-Sessoms et al., 2015) and the phosphate transporters
97 *PT4* (Javot et al., 2007) and *PT8* (Breuillin-Sessoms et al., 2015) are involved in the uptake of N
98 and P from the periarbuscular space between the fungal plasma membrane and the PAM. In
99 exchange, host plants transfer about 20% of their photosynthetically derived carbon to their fungal
100 partners, and these high carbon costs force host plants to strongly regulate the carbon flux to its
101 fungal symbionts (Wright et al., 1998). The host plant releases lipids and sugars into the
102 mycorrhizal interface likely via the putative lipid transporters *STR* and *STR2* (Zhang et al., 2010;
103 Roth and Paszkowski, 2017) and the bidirectional sugar transporter *SWEET1.2* (formerly
104 SWEET1b, An et al., 2019; Doidy et al., 2019).

105 AM fungi differ in the benefits that they provide for their host plant. The cooperative AM
106 fungus *Rhizophagus irregularis* 09 (Ri09) transfers more N and P to its host plant and contributes
107 to higher mycorrhizal growth responses than the less-cooperative fungus *Glomus aggregatum* 165
108 (Ga165; Fellbaum et al., 2014). Symbiosis with Ga165 is also more costly for the host plant
109 (measured as carbon costs per P transferred) than with Ri09, and *M. truncatula* preferentially
110 allocates more carbon to Ri09 than to Ga165 (Kiers et al., 2011). Collectively, these studies suggest
111 that carbon to nutrient exchange processes are driven by biological market dynamics, but the

112 molecular mechanisms that regulate these processes are largely unknown. Here, we examine the
113 physiological and transcriptomic responses of the host plant *M. trancatula* to colonization by Ri09
114 or Ga165 under N and P limitation to gain further insight into the molecular processes that trigger
115 the differential response of a host plant to high- and low benefit AM fungal partners.
116

117 **RESULTS**

118 **Colonization by *Rhizophagus irregularis* 09 leads to higher plant biomass and phosphorus**
119 **and nitrogen uptake than *Glomus aggregatum* 165**

120 We used a dual-compartment pot system to compare the overall benefit that Ga165 and Ri09
121 provided to *M. truncatula* (**Supplemental Fig. S1**). The colonization rates for both fungi were
122 comparable and exceeded 80% (**Supplemental Fig. S2**). Compared to non-mycorrhizal (NM)
123 plants, Ri09 colonization led to a higher shoot and root biomass, whereas Ga165 provided no
124 growth benefits (**Fig. 1A-B**). Both fungi increased P content (**Fig. 1C-D**) and concentration
125 (**Supplemental Fig. S3**) in the shoots and roots of their host, but Ri09 transferred more P than
126 Ga165. Nitrogen-15 (^{15}N) enrichment levels in the roots and shoots of NM plants did not exceed
127 natural abundance levels (**Fig. 1E-F**), which confirms that there was no mass flow of ^{15}N from the
128 HC into the RC. Both fungi transferred ^{15}N from the HC to their host, but Ga165 only increased
129 root ^{15}N enrichment, whereas Ri09 increased both root and shoot ^{15}N enrichment. Overall, these
130 data indicate that compared to Ga165, Ri09 promotes increased growth by providing its host plant
131 with greater access to both P and N.
132

133 **Colonization by either fungus alters global gene expression more dramatically in the roots**
134 **than in the shoots of *Medicago truncatula***

Figure 1

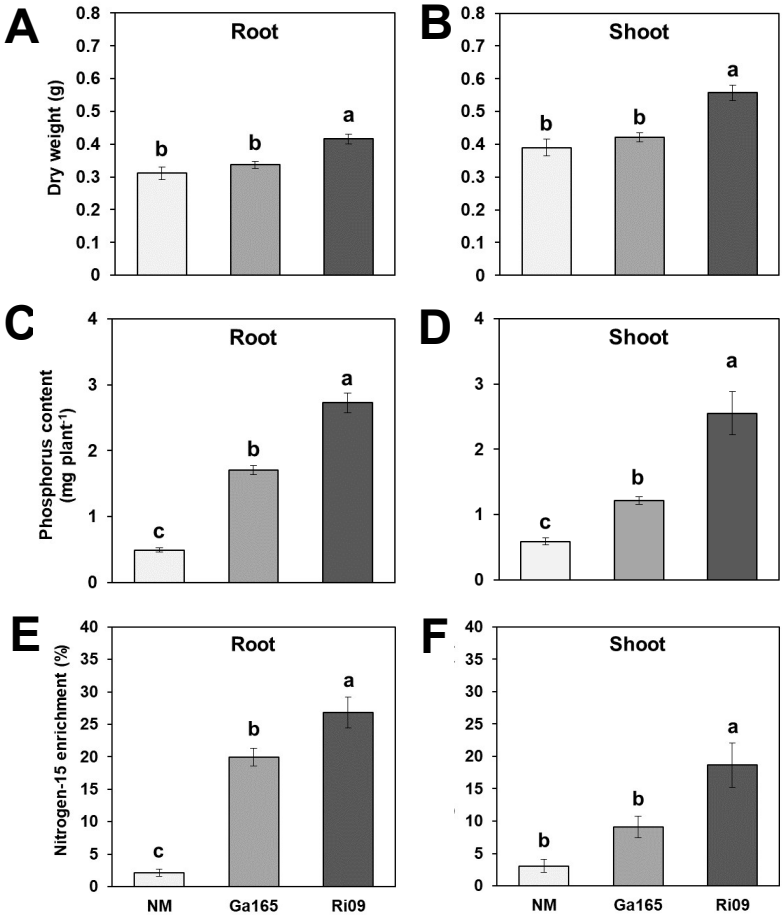

Figure 1. Biomass and nutrient content of *Medicago truncatula* plants colonized by different arbuscular mycorrhizal fungi. Shown are dry weight (A,B), phosphorus content (C,D), and % nitrogen-15 enrichment (E,F) of roots (left) and shoots (right). The plants were inoculated with either *Glomus aggregatum* 165 (Ga165) or *Rhizophagus irregularis* 09 (Ri09) and compared to non-mycorrhizal (NM) control plants. Bars represent the mean of each treatment (n = 5) ± SEM. Different letters on the bars indicate statistically significant ($p \leq 0.05$) differences based on one-way ANOVA and LSD test. F statistics and p-values are shown in Supplemental Table S1.

135 To identify potential molecular mechanisms responsible for the observed physiological responses,
136 we used RNA sequencing (RNA-seq) to evaluate global gene expression patterns in roots and
137 shoots of mycorrhizal and non-mycorrhizal plants. Analysis of the root data revealed distinct,
138 treatment-specific hierarchical clustering among biological replicates (n=3, Ga165 and NM; n=4,
139 Ri09) using a dendrogram, multidimensional scaling, and principal component analyses
140 (**Supplemental Fig. S4**). In contrast, analysis of the shoot data showed no distinct clustering
141 among biological replicates (n=4, Ga165 and NM; n=3, Ri09) within each treatment
142 (**Supplemental Fig. S5**), suggesting that only in the roots, global gene expression is driven by the
143 fungal partner. Consequently, the overall number of significant differentially expressed genes
144 (DEGs) was lower in the shoots than in the roots (**Supplemental Fig. S6**).
145

146 **Both shared and distinct sets of genes are differentially regulated in *Medicago truncatula* by**
147 **colonization with either fungus**

148 To identify key differences in the response of the host plant to both fungal species, we sorted all
149 DEGs from each treatment and used an arbitrary threshold of $\log_2$(fold-change) > 2 and a q-value
150 < 0.05 (**Fig. 2A**). In the roots, this threshold revealed that 364 genes were upregulated in roots
151 colonized by either fungus, and 197 or 165 genes were upregulated by colonization with only
152 Ga165 or Ri09, respectively (**Fig. 2B**). Ga165 and Ri09 colonization led to the downregulation of
153 41 shared genes, and 172 and 77 unique genes, respectively. The clustering of DEGs allowed us
154 to identify specific groups of similarly expressed genes (**Fig. 2C**). Clusters A and B are comprised
155 of genes that were strongly downregulated in mycorrhizal roots, cluster C1 contains genes that
156 were upregulated in mycorrhizal roots, clusters C2 and D include genes primarily upregulated by
157 Ga165 colonization, and cluster C3 contains genes exclusively upregulated by Ri09 colonization.

Figure 2

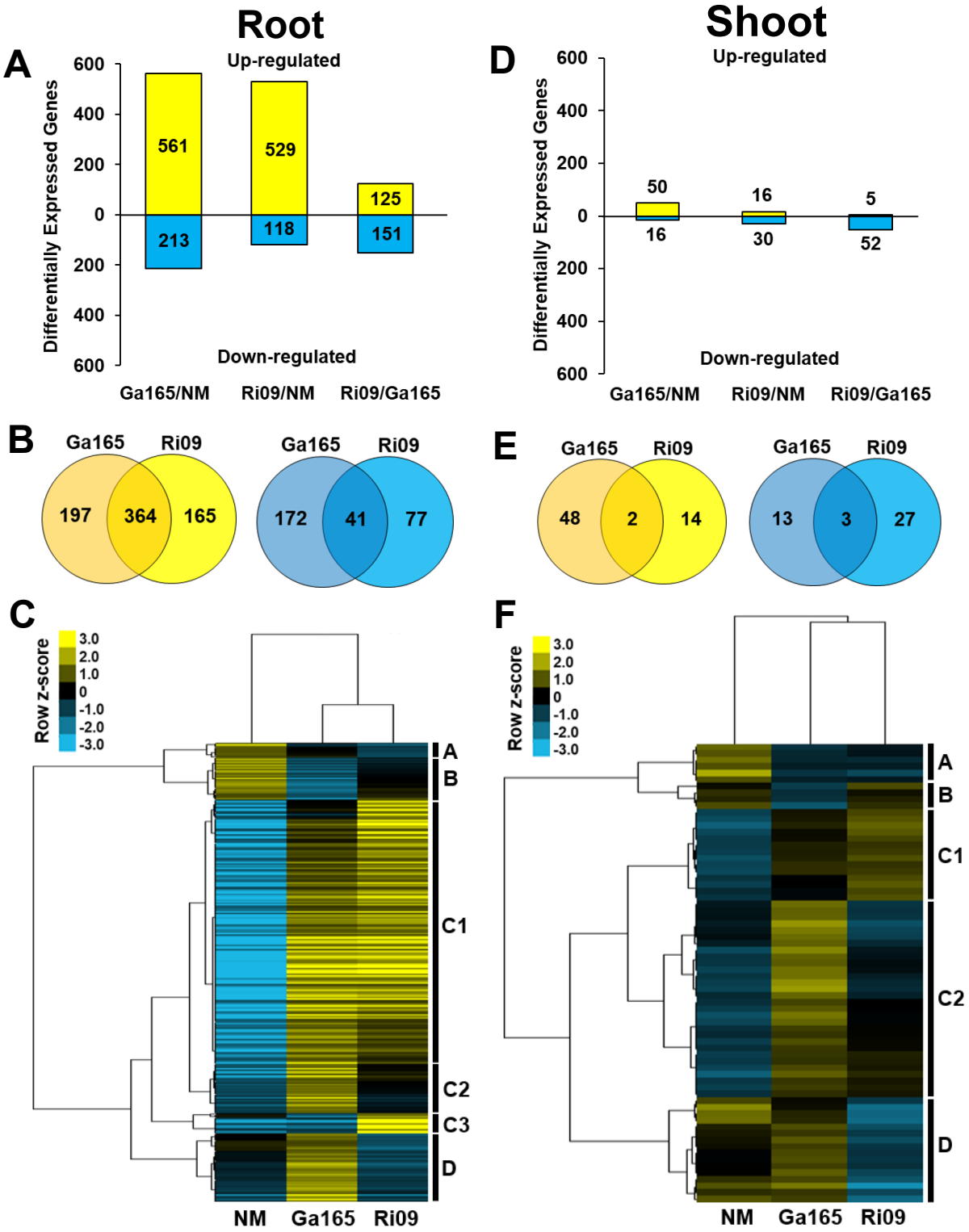

Figure 2. Significantly differentially expressed genes in roots (A–C) and shoots (D–F) of *Medicago truncatula* colonized by different AM fungi. (A, D) Number of significantly differentially expressed genes (DEGs; $\log_2$[fold-change] > 2 and a q-value < 0.05) in plants colonized by *Glomus aggregatum* 165 (Ga165) or *Rhizophagus irregularis* 09 (Ri09) compared either to non-mycorrhizal (NM) control plants or to each other. (B, E) Venn diagrams of significantly upregulated (yellow) and downregulated (blue) DEGs unique to Ga165 and Ri09-colonized plants or shared by both. (C, F) Heat maps of fragments per kilobase of transcript per million mapped reads (FPKM) values + 1 for all significant DEGs from each treatment. Gene clusters are assigned based on second-order branching. Upregulated genes are shown in yellow and downregulated genes in blue with intensity based on row z-score. All DEGs in each plot for roots and shoots are listed in Supplemental Files 1 and 2, respectively.

158 Although fewer genes were differentially expressed in the shoots, many were above our
159 applied threshold (**Fig. 2D**). We found that 48 and 14 genes were up, and 13 and 27 genes were
160 downregulated in the shoots of Ga165 and Ri09-colonized plants, respectively (**Fig. 2E**). In
161 contrast to the roots, clustering of DEGs based on expression patterns in the shoots (**Fig. 2F)**
162 revealed that only a small number of genes were upregulated (cluster C1) or downregulated (cluster
163 A) in mycorrhizal plants. In addition, some genes were only downregulated by Ga165 (cluster B)
164 or by Ri09 colonization (cluster D), while others were primarily upregulated by Ga165
165 colonization (cluster C2). Collectively, these results demonstrate that compared to shoots, gene
166 expression patterns in roots respond more strongly to colonization with different AM fungi, and
167 that both fungi lead to distinct differences in both root and shoot transcriptome profiles.
168

169 **Genes important for AM symbiosis are more strongly upregulated by *Rhizophagus***
170 ***irregularis* 09 than *Glomus aggregatum* 165**

171 We conducted a targeted analysis of the root RNA-seq data by first evaluating the expression of
172 key AM symbiosis genes (**Supplemental Table S2**). Among six core strigolactone biosynthesis
173 or exporter genes (**Fig. 3A**), we observed that two (*DXS2* and *D27*) were upregulated in AM roots
174 compared to the NM control; one (*MAX1a*) was only upregulated in Ri09-colonized roots, while
175 three (*CCD7*, *CCD8-1* and *PDR1a*) were not affected. Two GRAS transcription factors (*NSP1* and
176 *NSP2*) that regulate strigolactone biosynthesis and other symbiosis genes were also upregulated,
177 particularly in Ri09-colonized roots. The combined increased expression of *NSP1*, *NSP2*, *CCD7*,
178 and *MAX1a* (**Fig. 3B-E**) suggests that Ri09 more strongly induces strigolactone biosynthesis in
179 the roots than Ga165.

Figure 3

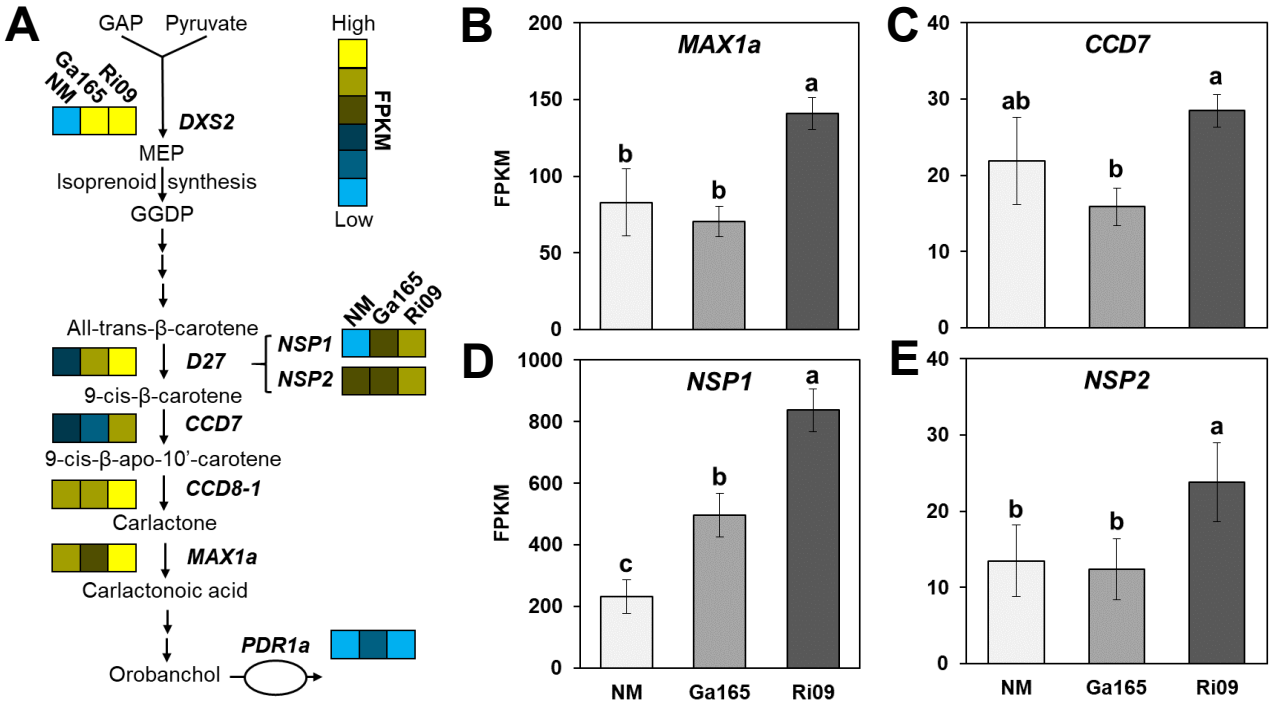

Figure 3. Expression patterns of genes in the strigolactone biosynthesis pathway. (A) Diagram of the strigolactone biosynthesis pathway and the relative expression levels of genes in *Medicago truncatula* that encode components of the pathway shown as fragments per kilobase of transcript per million mapped reads (FPKM; blue=low, yellow=high) in roots from non-mycorrhizal (NM) plants or plants colonized by either *Glomus aggregatum* 165 (Ga165) or *Rhizophagus irregularis* 09 (Ri09). The expression patterns (FPKM) for four specific genes upregulated by Ri09-colonization are also shown, including (B) *More Axillary Growth 1a* (*MAX1a*), (C) *Carotenoid Cleavage Dioxygenase 7* (*CCD7*), (D) *Nodulation Signaling Pathway 1* (*NSP1*) and (E) *NSP2* in NM roots (n=3) and roots inoculated with Ga165 (n=3) or Ri09 (n=4). Bars represent the mean of each treatment ± SEM. Significant differences (q-value < 0.05) in FPKM values between treatments were determined as part of the CuffDiff2 analysis and are indicated using different letters (see Supplemental Table S2). Abbreviations in A: GAP, glyceraldehyde 3-phosphate; DXS2, 1-deoxyxylulose 5-phosphate synthase2; MEP, 2-methyl-erythritol-4-phosphate; GGDP geranylgeranyl pyrophosphate; D27, Dwarf27; and PDR1a, pleiotropic drug resistance 1a.

180 Among the CSSP genes, the lipochitooligosaccharide receptor *NFP* was downregulated
181 and *PUB1*, a negative regulator of AM symbiosis, was upregulated in roots colonized by either
182 fungus (**Supplemental Table S2)**. None of the other 13 analyzed CSSP genes were affected.
183 Downstream of the CSSP, we evaluated the expression of 21 genes (**Supplemental Table S3**),
184 including: seven AM-induced transcription factors that regulate arbuscule development, function,
185 or degradation — *DIP1*, *RAD1*, *RAM1*, *MIG1*/*2*/*3*, and *MYB1*; three cellular remodeling genes —
186 *EXO70I*, *SYP132A*, and *VAPYRIN*; two phosphate transporters (*PT4* and *PT8*); three ammonium
187 transporters (*AMT2;3*, *AMT2;4*, and *AMT2;5*); the putative lipid transporters *STR* and *STR2* and
188 three lipid biosynthesis genes — *RAM2*, *FatM*, and *WRI5a*; and the sugar transporter *SWEET1.2*.
189 Almost all these genes were upregulated by both AM fungal species; however, six were
190 substantially more upregulated by Ri09, including: *RAD1*, *MYB1*, *PT8*, *AMT2;3*, *RAM2*, and
191 *SWEET1.2* (**Fig. 4A-F**). Together with the physiological results, the increased upregulation of
192 transporter genes in Ri09-colonized roots is suggestive of greater nutrient exchange activity across
193 the PAM in these roots.
194

195 **Gene ontology enrichment differs in the roots of *Medicago truncatula* when colonized by**
196 ***Glomus aggregatum* 165 or *Rhizophagus irregularis* 09**

197 We employed gene ontology (GO) enrichment analysis to identify cellular components, molecular
198 functions, and/or biological processes that were significantly enriched among genes that are only
199 upregulated (**Supplemental Fig. S7**) or downregulated (**Supplemental Fig. S8**) in AM roots.
200 Although we found many enriched GO terms, we only focus here on those associated with biotic
201 or abiotic stress and nutrient transport due to the key role that AM fungi play for these processes.
202 Among upregulated genes, the GO term "response to water deprivation" (GO:0009414; 6 genes)

Figure 4

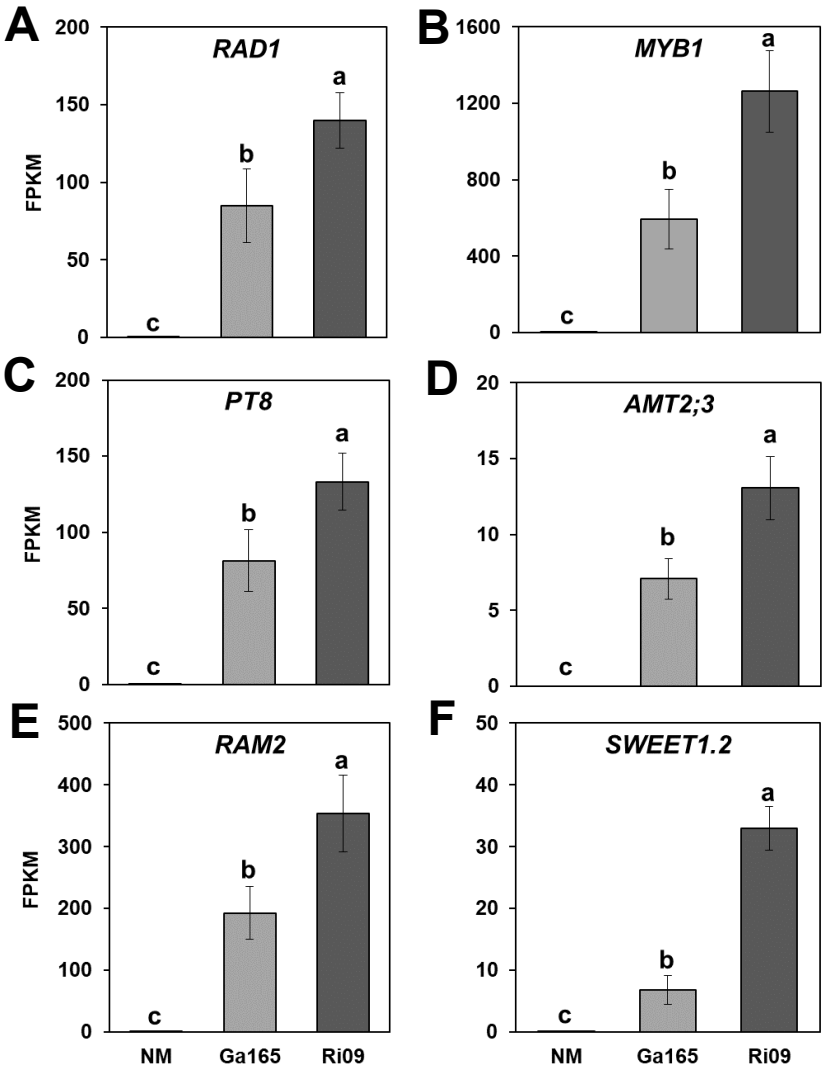

Figure 4. Relative expression of six genes in the roots of *Medicago truncatula* after colonization with different AM fungi. Expression of (A) *Required for Arbuscule Development 1* (*RAD1*), (B) *MYB-like Transcription Factor 1* (*MYB1*), (C) *Phosphate Transporter 8* (*PT8*), (D) *Ammonium Transporter 2;3* (*AMT2;3*), (E) *Reduced Arbuscular Mycorrhization 2* (*RAM2*), and (F) *Sugars Will Eventually Be Exported Transporter 1.2* (*SWEET1.2*) are shown for non-mycorrhizal plants (NM, n=3) and plants inoculated with *Glomus aggregatum* 165 (Ga165, n=3) or *Rhizophagus irregularis* 09 (Ri09, n=4). Expression levels are shown as fragments per kilobase of transcript per million mapped reads (FPKM). Bars represent the mean of each treatment ± SEM. Significant differences (q-value < 0.05) in FPKM values between treatments were determined as part of the CuffDiff2 analysis and are indicated using different letters (see Supplemental Table S3).

203 was enriched in Ga165-colonized roots (**Supplemental Fig. S7A**), while "defense response"
204 (GO:0006952; 11 genes) was enriched in Ri09-colonized roots (**Supplemental Fig. S7B**). The GO
205 terms "integral membrane components" (GO:0016021; 104 genes) and "modification of
206 morphology or physiology of other organism" (GO:00335821; 3 genes) were enriched by both
207 fungi (**Supplemental Fig. S7C**). Among down-regulated genes, the GO term "root hair
208 elongation" (GO:0008970, 3 genes) was enriched in Ga165-colonized roots (**Supplemental Fig.
209 S8A**).
210

211 **Colonization with *Glomus aggregatum* 165 and *Rhizophagus irregularis* 09 differentially
212 affect the expression of transporters**

213 Among upregulated genes, the GO terms "regulation of anion transmembrane transport"
214 (GO:1903959; 2 genes) and "anion transmembrane transporter activity" (GO:0008509; 5 genes)
215 were enriched in Ri09-colonized and AM-colonized roots, respectively (**Supplemental Fig. S7B-
216 C**). For downregulated genes, five GO terms related to transport were enriched in Ga165-colonized
217 roots (**Supplemental Fig. S8A**), but only two transport-related GO terms were enriched in Ri09-
218 colonized roots (**Supplemental Fig S8B**). The GO term "transmembrane transport" (GO:0055085;
219 five genes) was enriched by AM colonization (**Supplemental Fig. S8C**).

220 Given the dramatic difference in GO terms related to transport among Ga165 and Ri09-
221 colonized roots, we filtered all gene annotations containing the term "transport" from the *M.
222 truncatula* JCVI 4.0v2 annotation file (Tang et al., 2014) and found 259 genes that were
223 significantly differentially regulated in mycorrhizal roots (**Supplemental File 4**). Based on their
224 function, we further subdivided these genes into two groups: transport of mineral nutrients (72
225 genes) and secondary metabolites (187 genes). Compared to NM roots, 12 mineral transporters

226 were up- and 17 were down-regulated by both AM fungi (**Fig. 5A**). This suggests that a core set
227 of mineral transporters in AM roots are similarly regulated independent of fungal benefits.
228 However, a unique set of transporters were differentially regulated by each AM fungal species: 14
229 were up- and 13 were down-regulated in Ga165-colonized roots, while only 7 were up- and 12
230 were down-regulated in Ri09-colonized roots. From the identified 16 groups of mineral
231 transporters (**Fig. 5B**), we focused on ammonium, nitrate, phosphate, and sulfate transporters with
232 FPKM ≥ 10, due to the key role that AM fungi play in the transport of these nutrients (**Fig. 5C-F**).
233 Among the five differentially regulated ammonium transporters, one belongs to the AMT1
234 ammonium transporter family and four to the AMT2 family. Compared to AM roots, *AMT1;1* and
235 two of the AMT2 family transporters (*AMT2;1* and *AMT2;6*) were highly expressed in NM roots,
236 while *AMT2;3* and *AMT2;5* were specifically induced in mycorrhizal roots. *AMT2;3* was
237 particularly up-regulated in Ri09-colonized roots (**Fig. 5C**).

238 We also identified seven differentially regulated nitrate transporters (**Fig. 5D**). Five belong
239 to the nitrate/peptide transporter (NPF) family, and two are putative nitrate transporters.
240 Interestingly, the most highly expressed nitrate transporter (*NPF4.12*) was highly upregulated in
241 AM roots, particularly in Ri09-colonized roots. In contrast, five nitrate transporters were more
242 highly expressed in Ga165-colonized roots than in Ri09-colonized roots (*NPF1.2*, *NPF1.5*,
243 *NPF1.6*, *Medtr4g114340*, and *Medtr1g057460*), and two (*NPF1.2* and *Medtr1g057460*) also
244 differed from control roots. Only the nitrate transporter *NPF5.24* and *Medtr1g057460* showed
245 higher expression in NM roots than in either AM-colonized roots.

246 Seven phosphate transporters were differentially regulated (**Fig. 5E**). Four belong to the
247 high-affinity inorganic phosphate transporter family PHT1 (*PT4*, *PT6*, *PT8*, and *PT9*), two were
248 annotated as high-affinity inorganic phosphate transporters (*Medtr1g043290* and

Figure 5

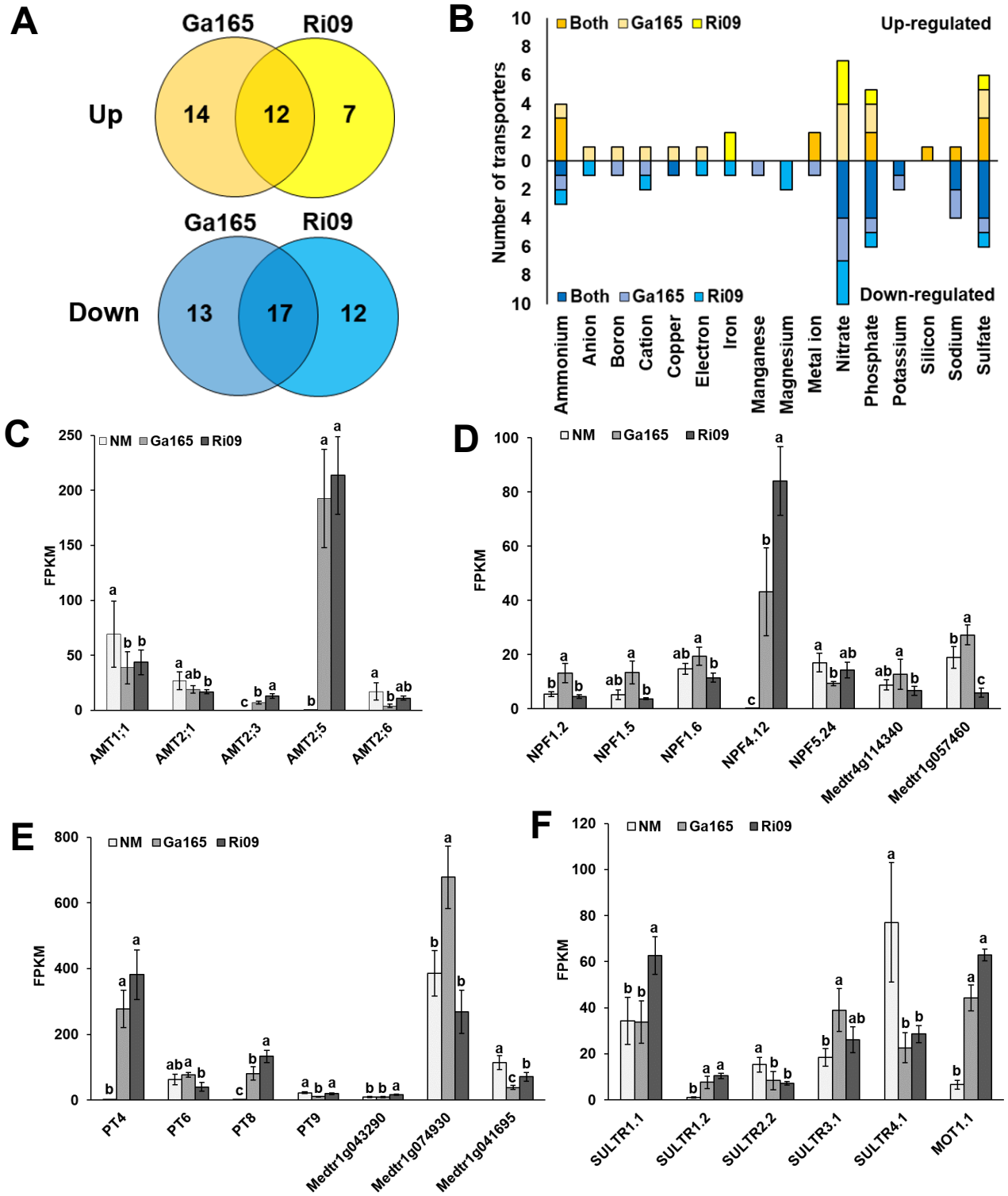

Figure 5. Expression patterns of significantly differentially expressed mineral transporter genes in the roots of *Medicago truncatula* after colonization with different AM fungi. (A) Venn diagrams showing the number of mineral transporters that are significantly up- (yellow) or down-regulated (blue) in roots colonized by *Glomus aggregatum* 165 (Ga165) or *Rhizophagus irregularis* 09 (Ri09), or both. (B) Summary of the number of genes from specific gene annotation groups of mineral transporters that are up- or down-regulated in roots colonized by Ga165 or Ri09, or both (see also Supplemental File 5). Expression patterns of genes annotated as (C) ammonium, (D) nitrate, (E) phosphate, and (F) sulfate transporters in the roots of non-mycorrhizal plants (NM) (n=3) and plants inoculated with Ga165 (n=3) or Ri09 (n=4). The bars in C–F represent the mean of each treatment ± SEM. Expression levels are shown as fragments per kilobase of transcript per million mapped reads (FPKM), only genes with FPKM ≥ 10 are shown, significant differences (q-value < 0.05) in FPKM values between treatments were determined as part of the CuffDiff2 analysis and are indicated using different letters on the bars.

249 *Medtr1g074930*), and one as a phosphate transporter PHO1-like protein. As expected, two of the
250 PHT1 transporter genes, *PT4* and *PT8*, were only expressed in AM roots, and *PT8* expression was
251 higher in Ri09-colonized roots. By contrast, the expression of *Medtr1g074930* was strongly
252 upregulated in Ga165-colonized roots compared to NM and Ri09-colonized roots. The PHO1-like
253 transporter (*Medtr1g041695*) showed higher expression levels in NM than in AM roots.

254 We identified six sulfate transporters that were differentially regulated among the three
255 treatments (**Fig. 5F**). Two were annotated as high affinity sulfate transporter 1 (SULTR1) family
256 genes (*SULTR1.1* and *1.2*), three as sulfate/bicarbonate/oxalate exchanger and transporter genes
257 (*SULTR2.2*, *3.1*, and *4.1*), and one as a sulfate transporter-like gene (*MOT1.1*). While the
258 expression levels of *SULTR2.2* and *SULTR4.1* were higher in NM roots than in AM roots, the
259 remaining sulfate transporters were upregulated by colonization with Ri09 (*SULTR1.1*), Ga165
260 (*SULTR3.1*), or by both fungi (*SULTR1.2* and *MOT1.1*).

261 In total, we identified 20 groups of secondary metabolite transporters in our dataset.
262 Compared to NM control roots, 29 of these transporters were up- and 43 were downregulated in
263 AM roots (**Fig. 6A**). Several secondary metabolite transporters were differentially regulated in
264 Ga165 and Ri09-colonized roots. Among these, most belonged to six gene annotation groups,
265 including ATP-binding cassette (ABC), amino acid, major facilitator superfamily (MFS), major
266 intrinsic protein (MIP), peptide, and Sugars Will Eventually be Exported Transporters (SWEETs)
267 (**Fig. 6B**). Here, we will only discuss those transporters that are known to play a role in AM
268 symbiosis, or that were strongly differentially regulated by mycorrhizal colonization, but have not
269 yet been functionally characterized.

270 Two white-brown-complex ABC transporter family proteins (*STR* and *STR2*; Zhang et al.,
271 2010), three ABC transporter B family proteins (*AMN2*, *AMN3* [Roy, 2015], and *Medtr4g124040*),

272 and one drug resistance transporter-like ABC domain protein (*Medtr1g050525*) were strongly
273 upregulated in AM roots, particularly in Ri09-colonized roots (**Fig. 6C**). The expression levels in
274 Ga165-colonized roots were higher but did not always differ significantly from the NM roots.

275 Two amino acid transporters, *Medtr1g030660* and *Medtr2g101920*, and two peptide
276 transporters, *PTR3* and *OPT15*, were upregulated in mycorrhizal roots (**Fig. 6D**). As expected,
277 *NOPE1,* an N-acetylglucosamine transporter of the major facilitator superfamily (MFS) that is
278 required for AM symbiosis (Nadal et al., 2017), was also highly upregulated in AM roots (**Fig.**
279 **6E**). Three major intrinsic protein (MIP) transporters, *NIP1;5*, *NIP1;6*, and *NIP3;1*, which are
280 often classified as aquaporins, were all upregulated in mycorrhizal roots. *NIP1;5* was particularly
281 highly expressed in Ri09-colonized roots, while *NIP1;6*, *NIP3;1* and *NIP6;2* showed higher
282 expression levels in Ga165-colonized roots.

283 SWEETs are known to play a crucial role in AM symbiosis (Doidy et al., 2019), and five
284 were differentially expressed in AM roots. *SWEET1.2* was upregulated by colonization with either
285 fungus, but especially with Ri09. *SWEET3.3* and *SWEET12,* were only upregulated in Ri09-
286 colonized roots, whereas *SWEET7* and *SWEET13* were only upregulated in Ga165-colonized roots
287 (**Fig. 6F**). The variation in the expression patterns of these five *SWEET* genes suggests that sugar
288 transport is strongly regulated in response to fungal benefit.

289

290 **Photosynthesis-related genes in the shoots are upregulated in response to colonization with**
291 ***Rhizophagus irregularis* 09**

292 To identify gene groups that were differentially expressed in the shoots of mycorrhizal plants, we
293 performed GO enrichment analysis on several gene clusters shown in **Fig. 2F**. Due to the low
294 number of genes, the analysis could not be completed for clusters A and B; also, given the large

Figure 6

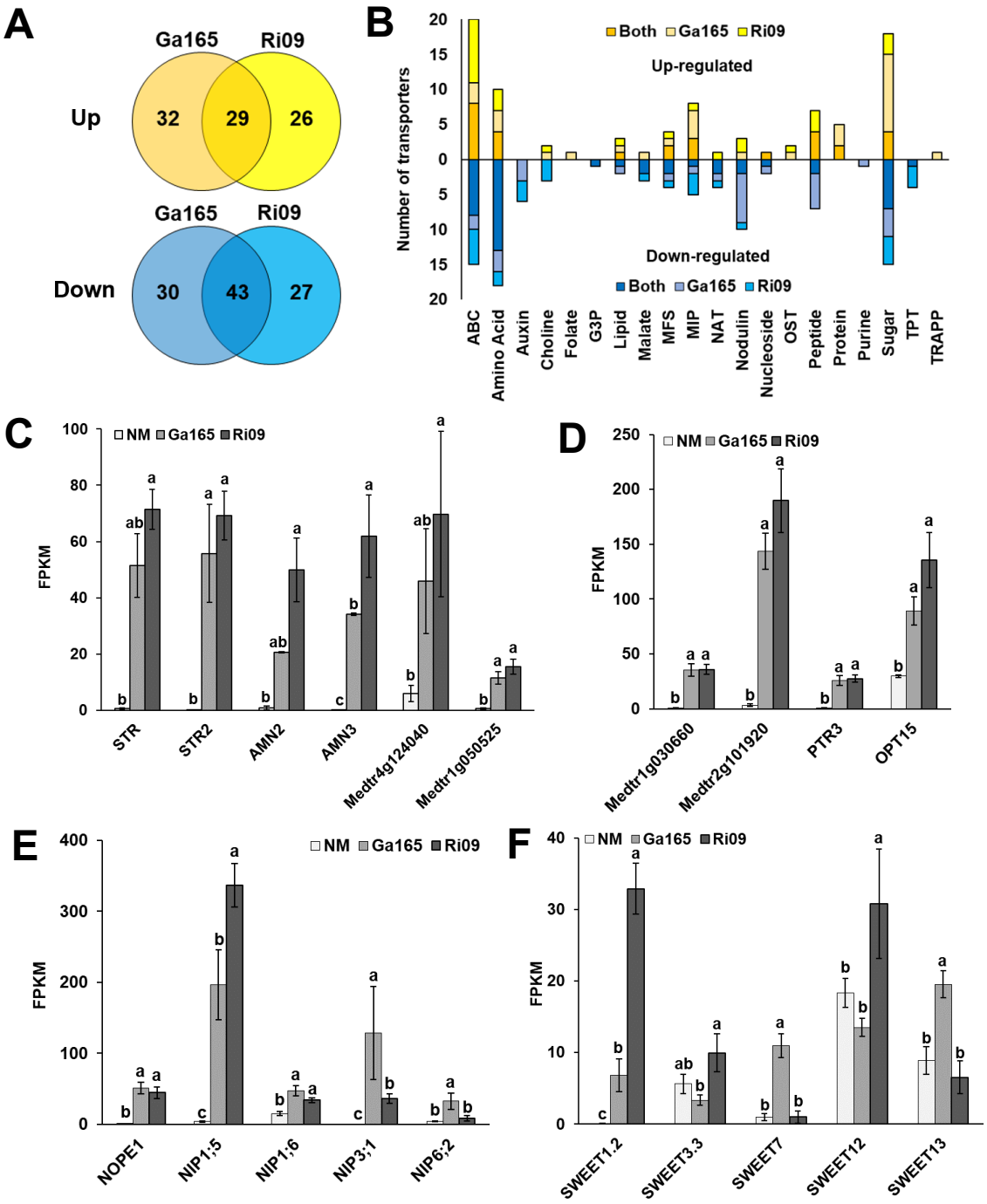

Figure 6. Expression patterns of significantly differentially expressed secondary metabolite transporters in the roots of *Medicago truncatula* after colonization with different AM fungi. (A) Venn diagrams showing the number of secondary metabolite transporters that are significantly up- (yellow) or down-regulated (blue) in roots colonized by *Glomus aggregatum* 165 (Ga165) or *Rhizophagus irregularis* 09 (Ri09), or both. (B) Summary of the number of genes from specific gene annotation groups of secondary metabolite transports that are up- or down-regulated in roots colonized by Ga165 or Ri09, or both (see Supplemental File 6). Expression patterns of genes annotated as (C) ATP-binding cassette (ABC), (D) amino acid or peptide, (E) major facilitator superfamily (MFS) or major intrinsic protein (MIP), and (F) sugar transporters in the roots of non-mycorrhizal plants (NM) (n = 3) and plants inoculated with Ga165 (n =3) or Ri09 (n = 4). The bars in C-F represent the mean of each treatment ± SEM. Expression levels are shown as fragments per kilobase of transcript per million mapped reads (FPKM); only genes with FPKM ≥ 10 are shown; significant differences (q-value < 0.05) in FPKM values between treatments were determined as part of the CuffDiff2 analysis and are indicated using different letters on the bars. Abbreviations in B: G3P, glycerol-3-phosphate; NAT, nucleobase-ascorbate transporter; OST, organic solute transporter; TPT, triose-phosphate transporter; TRAPP, transport protein particle.

295 number of genes in cluster C, we divided the cluster into two groups dependent on whether the
296 genes were upregulated by Ri09 (cluster C1, **Supplemental Fig. S9A**) or by Ga165 colonization
297 (cluster C2, **Supplemental Fig. S9B**). In addition, we performed GO enrichment analysis with the
298 cluster D genes which are downregulated in Ri09-colonized plants (**Supplemental Fig. S9C**).
299 The GO terms that were enriched in the shoots of Ri09-colonized plants were cellular
300 components and biological processes associated with photosynthesis (**Supplemental Fig. S9A**).
301 The five genes linked with these GO terms were annotated as follows: *Medtr1g115410*,
302 photosystem II reaction center family protein (orthologous to PsbP in *Arabidopsis thaliana*);
303 *Medtr2g082580*, oxygen-evolving enhancer protein (orthologous to PsbQ-like protein 2 in *A.*
304 *thaliana*); *Medtr5g018670*, photosystem II oxygen-evolving enhancer protein; *Medtr1g015290*,
305 ultraviolet-B-repressible protein (orthologous to PsbX in *A. thaliana*); and *Medtr1588s0010*, ATP
306 synthase F1, gamma subunit. The expression levels of *PsbP*, *PsbQ-like protein 2*, *PsbX*, and the
307 ATP synthase gene were significantly higher in the shoots of Ri09-colonized plants than in NM
308 plants (**Fig. 7A**). Out of these genes, only PsbP was also significantly upregulated in Ga165-
309 colonized plants. By contrast, *Medtr5g018670* was more highly expressed in the shoots of Ga165-
310 colonized than in NM plants. Overall, these expression patterns imply that photosynthesis was
311 more strongly induced in Ri09-colonized plants.
312

313 **Biotic and abiotic stress-related genes are differentially regulated in the shoots of *Glomus***
314 ***aggregatum* and *Rhizophagus irregularis* colonized plants**

315 Many of the GO terms that were enriched in the shoots of Ga165-colonized plants encompassed
316 biological processes related to biotic stresses, including: “response to wounding” (GO:0009611),
317 “defense response to fungus” (GO:0050832), and “defense response to bacterium” (GO:0042742)

318 (**Supplemental Fig. S9B**). The genes linked to these GO terms were annotated as:
319 *Medtr4g054920*, cytochrome P450 family 94 protein; *Medtr4g120760*, pathogenesis-related
320 protein bet V I family protein; *Medtr8g096900,* pathogenesis-related thaumatin family protein;
321 *Medtr4g092010*, (3S)-linalool/(E)-nerolidol/(E,E)-geranyl linalool synthase; and *Medtr5g053950*,
322 allene oxide cyclase. The fact that these GO terms were only enriched in Ga165-colonized plants
323 suggests that the host plant responds to Ga165 as it would to a pathogen by upregulating defense
324 responses (**Fig. 7B**).

325 In contrast, Ri09 colonization led to the down-regulation of genes (**Fig. 2F**, cluster D),
326 associated with three GO terms: "response to hydrogen peroxide" (GO:0042542), "response to
327 abiotic stimulus" (GO:0009628), and "response to bacterium" (GO0009617) (**Supplemental Fig.
328 S9C**). The genes included in these GO terms were annotated as: *Medtr1g048990*, superoxide
329 dismutase; *Medtr7g069980*, ferritin; *Medtr8g059170*, NAC transcription factor-like protein;
330 *Medtr7g079180*, late embryogenesis abundant protein; and *Medtr3g087590*, myo-inositol 1-
331 phosphate synthase. The expression of *Medtr7g079180* was upregulated by both fungi, but the
332 remaining abiotic stress response genes were more highly expressed in NM or Ga165-colonized
333 plants than in Ri09-colonized plants (**Fig. 7C**). Collectively, the expression patterns of these
334 abiotic stress response genes could indicate that Ri09 is more effective at conferring abiotic stress
335 tolerance to *M. truncatula* than Ga165.

336

337 **DISCUSSION**

338 **The growth and nutritional benefits of arbuscular mycorrhizal fungi are linked to**
339 **mycorrhiza-induced transporter expression**

Figure 7

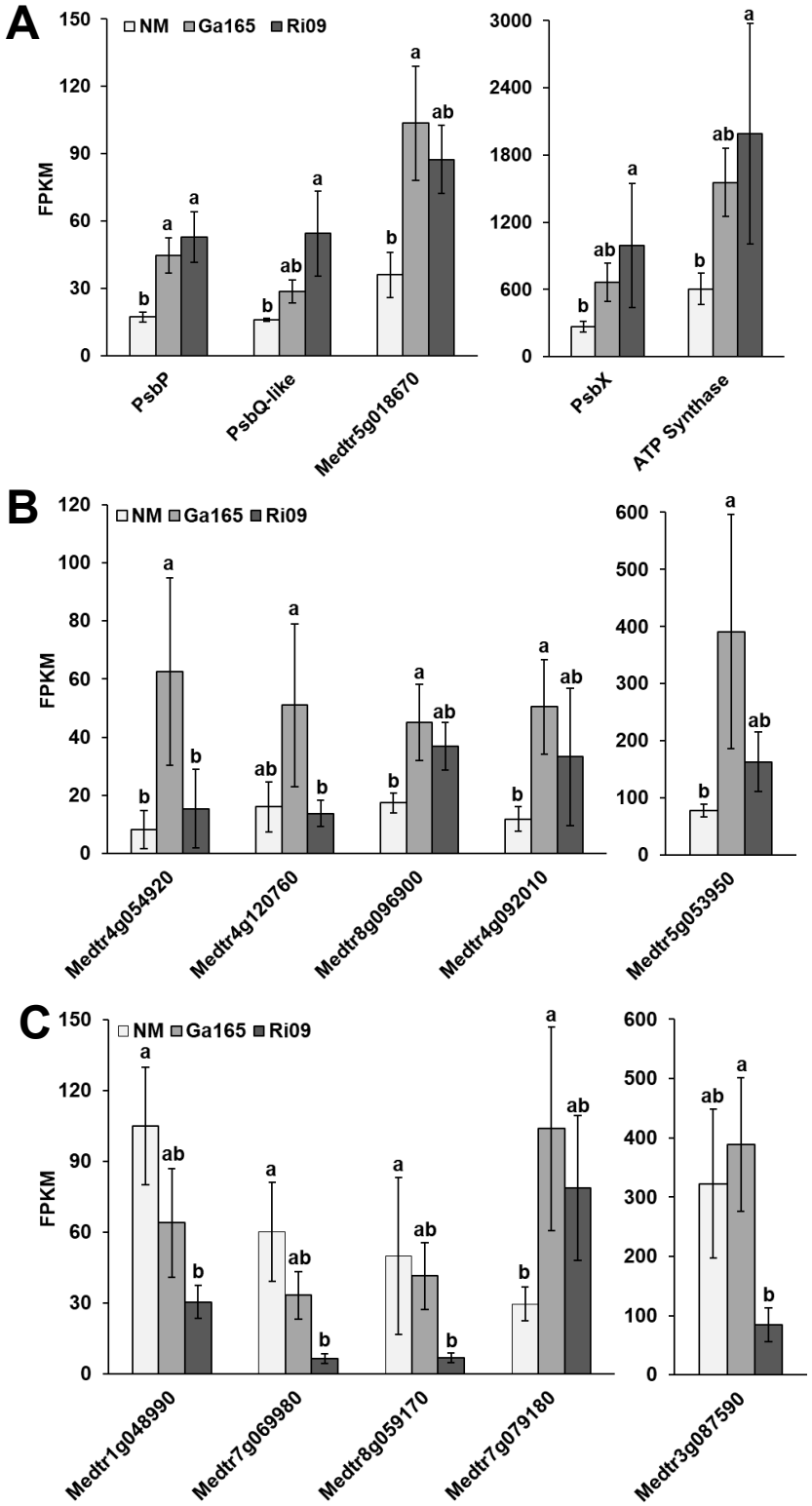

Figure 7. Expression patterns of significantly differentially expressed genes in the shoots of *Medicago truncatula* colonized by different AM fungi. Expression levels of genes involved in (A) photosynthesis, (B) response to biotic stress, and (C) response to abiotic stress in non-mycorrhizal plants (NM; n=4) or plants colonized by *Glomus aggregatum* 165 (Ga165, n=4) or *Rhizophagus irregularis* 09 (Ri09, n=3). Bars represent the mean of each treatment ± SEM. Expression levels are shown as fragments per kilobase of transcript per million mapped reads (FPKM), and significant differences (q-value < 0.05) in FPKM values between treatments were determined as part of the CuffDiff2 analysis and are indicated using different letters above the bars (see also Supplemental Table S4).

340 When compatible host plants are inoculated with AM fungi, colonization most often leads to
341 increased growth and nutrient uptake, especially in nutrient-deprived conditions (Chandrasekaran,
342 2020). We found that under N and P limitation, Ri09 promoted greater growth and provided more
343 N and P to *M. truncatula* than Ga165 (**Fig. 1**). This observation is consistent with previous findings
344 where we demonstrated that Ri09 is more cooperative than Ga165 (Kiers et al., 2011; Fellbaum et
345 al., 2014; Wang et al., 2016) and with the expression patterns of mycorrhiza-induced N and P
346 transporters. For example, the known AM-induced ammonium transporters *AMT2;3* and *AMT2;5*
347 were upregulated by Ga165 and Ri09 (**Fig. 5C**). The expression levels of *AMT2;3* in AM roots
348 were lower than that of *AMT2;5*, but *AMT2;3* expression was more strongly upregulated by Ri09
349 than by Ga165 colonization. We also found that *NIP1;5* is strongly AM-induced (**Fig. 6E**), and
350 while its role in the AM symbiosis has not yet been characterized, the soybean ortholog *Nod26*
351 plays a crucial role in ammonium transport in the rhizobia-legume symbiosis (Frare et al., 2018).
352 Although the AM fungi were provided with $^{15}NH_4Cl$ as a N source, we also found that the nitrate
353 transporter *NPF4.12* was strongly induced in AM roots, especially in Ri09-colonized roots (**Fig.**
354 **5D**). Aloui et al. (2018) found that *NPF4.12* is enriched in the proteome of mycorrhizal *M.*
355 *truncatula* roots, and recently the rice ortholog *OsNPF4.5* was functionally characterized as an
356 AM-induced nitrate transporter (Wang et al., 2020). The stronger expression of ammonium and
357 nitrate transporters in Ri09 colonized roots aligns with the observed ^{15}N increase in the shoots of
358 Ri09-colonized plants.

359 The AM-induced P transporters *PT4* and *PT8* were both highly expressed in AM colonized
360 roots, especially Ri09-colonized roots (**Fig. 5E**). Similarly, colonization with both fungi, but
361 particularly with Ri09, caused an increase in shoot P content. However, *Medtr1g074930*, a putative
362 high affinity inorganic phosphate transporter, was strongly upregulated in Ga165-colonized roots

363 (**Fig. 5E**). This P transporter is upregulated during P deficiency (Wang et al., 2017); as such, the
364 upregulation of *Medtr1g074930* in our study could indicate that colonization by Ga165 resulted in
365 P deficiency in the host plant; but, this does not appear to be the case as *Medtr1g074930* was not
366 upregulated in the roots of NM plants (**Fig. 5E**) and Ga165-colonized roots had a higher P
367 concentration than NM roots (**Supplemental Fig. S3**). Regardless, others have similarly observed
368 that the expression of high affinity P transporters are differentially regulated in the host by
369 colonization with different species of AM fungi (Grunwald et al., 2009).

370 Like N and P, AM fungi also play a critical role in supplying sulfur to the host plant (Sieh
371 et al., 2013). We observed an upregulation of two sulfate transporters, *SULTR1.1* and *SULTR1.2*
372 (**Fig. 5F**). Both are upregulated in mycorrhizal *M. truncatula* roots, although not consistently
373 (Casieri et al., 2012; Wipf et al., 2014). The *SULTR1.2* ortholog in *Lotus japonicus* appears to play
374 an important role in both direct and mycorrhizal sulfur uptake pathways, and its promoter is active
375 in arbuscule-containing cells (Giovannetti et al., 2014). We also observed that the putative sulfate
376 transporter gene *MOT1.1* was upregulated in Ga165 and Ri09-colonized roots (**Fig. 5F**). However,
377 the involvement of MOT1.1 in sulfur transport has not been experimentally demonstrated yet, but
378 it is phylogenetically related to *MOT1.3*, which is a molybdate transporter crucial for the rhizobia-
379 legume symbiosis (Tejada-Jiménez et al., 2017).

380

381 **Patterns of photosynthesis, carbon transporter, and lipid biosynthesis gene expression in the**
382 **host plant are linked to the nutritional benefits provided by the fungal symbiont**

383 In exchange for the nutritional benefits, plants transfer between 4 and 20% of their net fixed carbon
384 in form of carbohydrates and lipids to their fungal symbiont (Wright et al., 1998; Roth and
385 Paszkowski, 2017). However, both the nutritional benefits that AM fungi provide and the increased

386 carbon sink they create are known to stimulate an increase in photosynthesis (Kaschuk et al., 2009).
387 In line with this, we observed that the expression levels of photosynthesis-related genes were more
388 strongly induced in Ri09- than in Ga165-colonized plants (**Fig. 7A**); thus, the elevated growth
389 response provided by Ri09 (**Fig. 1A-B**) was not only due to increased nutrient transfer, but also
390 likely due to an increase in photosynthesis.

391 Our previous studies have shown that host plants preferentially allocate more carbon to the
392 more cooperative AM fungus Ri09 (Kiers et al., 2011). Yet, we found that the putative lipid
393 transporters *STR* and *STR2* were upregulated in AM roots, but did not differ significantly between
394 Ga165 and Ri09-colonized roots (**Fig. 6C**). Nevertheless, we did observe that the expression levels
395 of the lipid biosynthesis gene *RAM2* (**Fig. 4**) and the sugar transporter *SWEET1.2* (**Fig. 6F**) were
396 higher in Ri09-colonized roots, which is suggestive of increased transport of carbon resources to
397 the fungus in exchange for elevated nutritional benefits (Bravo et al., 2017; An et al., 2019).(An
398 et al., 2019)

399 Although *SWEET1.2* is highly upregulated during AM colonization, particularly in
400 arbuscule-containing cortical cells, it is not essential for the maintenance of the AM symbiosis,
401 most likely because of functional redundancy between SWEET1.2 and other SWEETs (An et al.,
402 2019). We found that *SWEET3.3* and *SWEET12* were more strongly upregulated in Ri09-colonized
403 roots (**Fig. 6F**); both are upregulated in arbuscule-containing cortical cells in *M. truncatula*
404 (Sameeullah et al., 2016). Interestingly, *SWEET7* and *SWEET13* were more strongly induced in
405 Ga165-colonized roots, but SWEETs perform diverse physiological functions, and their
406 upregulation does not necessarily increase sugar transport to the fungus. For example, some
407 SWEET transporters in *Arabidopsis* localize to the tonoplast and restrict sugar efflux from the root
408 (Chen et al., 2015). Given the variable expression patterns of these five SWEETs in Ri09 and

409 Ga165-colonized roots and the varying roles they may play in sugar efflux and retention,
410 functionally characterizing them will improve our understanding of the mechanisms controlling
411 carbon allocation during AM symbiosis.
412

413 **Arbuscule development is regulated by the host based on the nutritional benefit of the**
414 **symbiont**

415 Based on the elevated expression levels of known mycorrhiza-induced transporters that localize to
416 the PAM (*PT8*, *AMT2;3*, and *SWEET1.2*) and of two genes involved in regulating arbuscular
417 development and degeneration (*RAD1* and *MYB1*) (**Fig. 4**), we hypothesized that these expression
418 levels might be linked to increased arbuscule abundance and size in Ri09-colonized roots, which
419 would increase the surface of the mycorrhizal interface. To test this, we conducted a short-term
420 experiment and examined the number and average size of arbuscules in Ri09- and Ga165-
421 colonized roots when arbuscules begin to form. Even in this short-term experiment, growth
422 differences among the different treatments were already clearly visible (**Fig. 8A**). We found that
423 Ri09 colonized the roots faster and formed more and larger arbuscules than Ga165 (**Fig. 8C-G**;
424 **Supplemental Fig. S10**), suggesting a greater surface area of the PAM in Ri09 than in Ga165-
425 colonized roots. A similar reduction in arbuscule size was observed previously in *mtpt4* mutants
426 (Javot et al., 2007). Thus, our results strongly indicate that the host is rewarding Ri09 but likely
427 sanctioning Ga165 based on the nutritional benefits that they provide.
428

429 **Arbuscular mycorrhiza-induced changes in the expression of host abiotic and biotic stress**
430 **response genes are species specific**

Figure 8

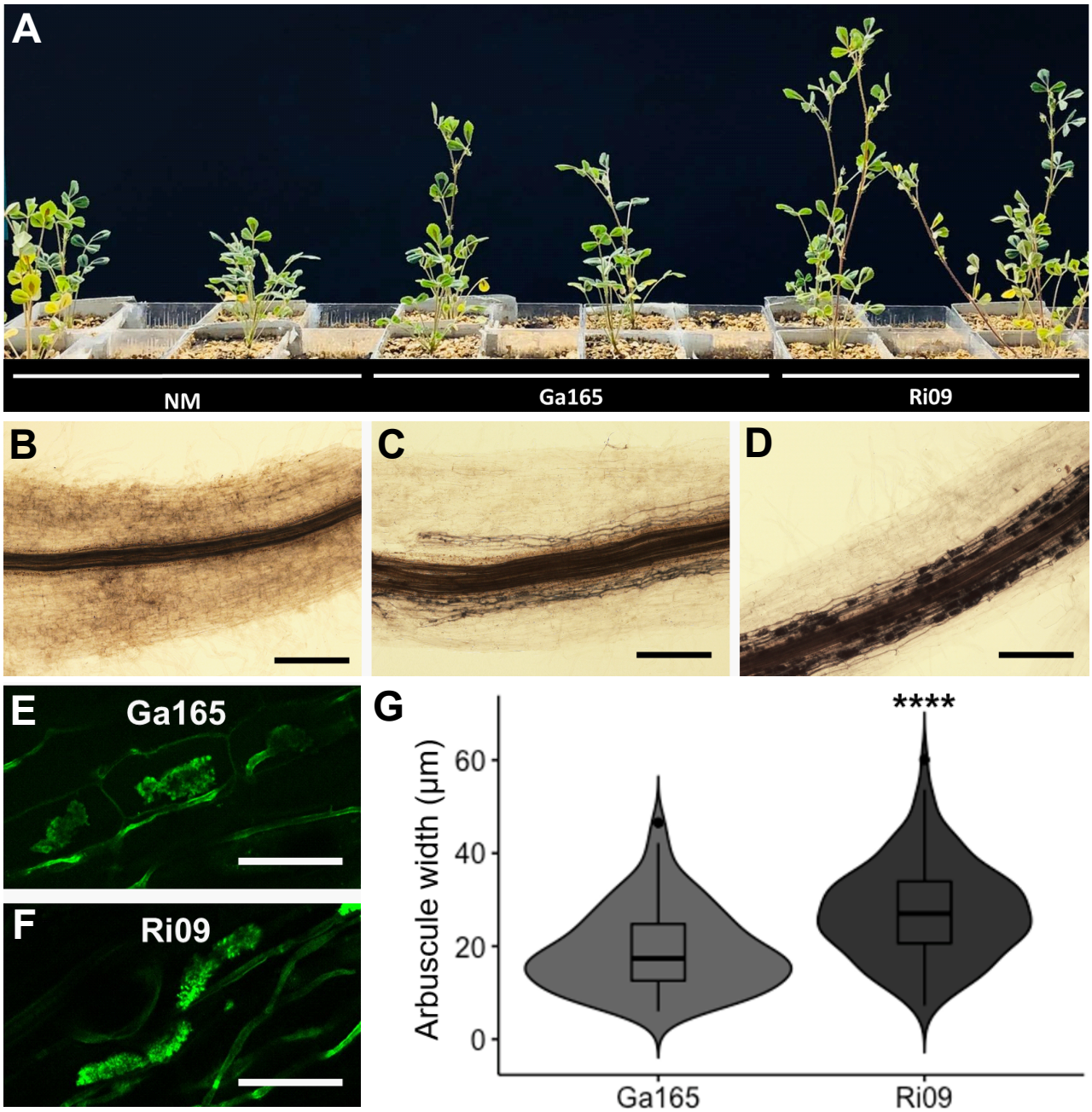

Figure 8. Colonization patterns and arbuscule size of *Glomus aggregatum* 165 and *Rhizophagus irregularis* 09 in *Medicago truncatula* roots three weeks post-inoculation. (A) Image of non-mycorrhizal *M. truncatula* plants compared to either *G. aggregatum* 165 (Ga165) or *R. irregularis* 09 (Ri09) colonized plants. (B–D) Representative images of ink-stained NM roots (B), Ga165-colonized roots (C), and Ri09-colonized roots (D) (scale bar = 200 µm). (E–F) Representative confocal images of Ga165 (E) and Ri09-colonized (F) roots containing arbuscules and stained with wheat germ agglutinin Alexafluor-488 (scale bar = 50 µm). (G) Box and whisker plots embedded in violin plots displaying the size distribution for the width of all arbuscules in Ga165 (light grey) and Ri09 (dark grey) colonized roots. In 11 and 15 colonized roots, 132 and 80 arbuscules were evaluated for Ga165 and Ri09, respectively. The mean arbuscule width for each fungal species was compared using a student's t-test (****$p < 0.0001$).

431 Although the primary focus of this study was to evaluate both resource exchange and transporter
432 expression, the global gene expression data also provided some unique insights into biotic and
433 abiotic stress responses. Mycorrhizal growth responses are context-dependent and fall along a
434 mutualism to parasitism continuum (Johnson and Graham, 2013). In natural environments, plants
435 are colonized by communities of AM fungi, which supports the idea of functional
436 complementarity, where a host plant experiences a broad range of benefits that are provided by
437 specific members of the AM fungal community (*e.g.*, enhanced nutrient availability or increased
438 disease resistance; Jansa et al., 2008). While Ga165 does not seem to provide sufficient nutritional
439 benefits to elicit a positive growth response, it is possible that like other AM fungal species it may
440 provide resistance to one or more abiotic stresses (e.g., salinity or heavy metal accumulation), none
441 of which were evaluated in this study.

442 For example, Ga165 more strongly up-regulated defense-response genes in the shoots (**Fig.**
443 **7B**), two of which (*Medtr4g120760* and *Medtr8g096900*) are upregulated in alfalfa when
444 challenged with the foliar fungal pathogen *Phoma medicaginis* (Li et al., 2019a) and pea aphids
445 (*Acyrthosiphon pisum*; Li et al., 2019b). As such, Ga165 may be more effective than Ri09 at
446 priming host defense responses thereby preventing infection from pathogens and mitigating
447 arthropod attack as has been described previously for other AM fungal species (Liu et al., 2007;
448 Sharma et al., 2017).

449 We also observed that genes associated with the GO term "response to water deprivation"
450 (GO:0009414; 6 genes) were upregulated in Ga165-colonized roots (**Supplemental Fig. S7A)**.
451 Three of these genes — *Medtr5g063670*, *Medtr7g093170*, and *Medtr8g026960* — were very
452 strongly upregulated and are annotated as annexin D8, seed maturation protein, and homeobox
453 associated leucine zipper protein, respectively. Although the precise role of annexin D8 is not

454 known, other annexins are differentially regulated during various abiotic and biotic stresses, and
455 some seem to play a role during AM symbiosis (Roux et al., 2012). The seed maturation protein
456 *Medtr7g093170* has been characterized as the late embryogenesis abundant protein LEA1370,
457 which is upregulated under various abiotic stresses, including abscisic acid treatment, cold, salinity
458 and dehydration (Zhang et al., 2020). Finally, the homeobox associated leucine zipper protein
459 encoded by *Medtr8g026960* was characterized as a transcription factor that is upregulated during
460 salt stress in alfalfa (Postnikova et al., 2013). However, since these genes are not yet functionally
461 characterized, the question whether Ga165 colonization could contribute to an alleviation of these
462 abiotic stresses, or whether host plants respond similarly to abiotic stress and to Ga165
463 colonization, requires further studies.

464 It is also possible that Ga165 truly is a low-benefit symbiont capable of persisting in a
465 community with high benefit AM fungi thereby avoiding both detection and subsequent
466 sanctioning by the host plant for poor performance (Hart et al., 2013). Avoiding detection could
467 be carried out using effectors, as has been described in the model AM fungus *R. irregularis*
468 DAOM197198 that counteracts the plant immune program with the small, secreted peptide SP7
469 (Kloppholz et al., 2011). Indeed, in our root expression data we observed that 11 defense response
470 genes, including three defensins (*Medtr8g012810, Medtr8g012815*, and *Medtr8g012845*) were
471 strongly up-regulated in Ri09, but not in Ga165-colonized roots (**Supplemental Fig. S7B**,
472 **Supplemental Table S5**). Defensins are known to inhibit pathogen growth (Maróti et al., 2015),
473 so it is tempting to speculate that Ga165 could temper host defense responses to avoid detection
474 and sanctioning. However, the defensin *DefMd1* when overexpressed upregulates the expression
475 of the GRAS transcription factor *RAM1*, which plays a critical role in arbuscule branching (Park

476 et al., 2015; Uhe et al., 2018). *RAM1* was highly upregulated in Ga165 and Ri09 colonized roots
477 suggesting that defensins might have a role in AM symbiosis.
478
479 **Global analysis of transporter expression in *Medicago truncatula* roots revealed interesting**
480 **candidates for future functional characterization**
481 This study has provided novel insights into the physiological and transcriptomic response of a host
482 plant to colonization by both high and low benefit AM fungi and **Fig. 9** provides an overview of
483 these responses. The experimental approach allowed us to identify both the molecular mechanisms
484 controlling the physiological responses we observed and transporters that are both commonly and
485 uniquely regulated by high (Ri09) and low benefit (Ga165) AM fungal strains. While the primary
486 focus of our study is on N, P, and carbon transporters in the roots of *M. truncatula* colonized by
487 Ga165 or Ri09, our global analysis of all differentially expressed transporters uncovered some
488 interesting gene candidates with unique expression patterns (**Figs. 5** and **6**). Although there was a
489 core set of transporters similarly induced by both fungi, a smaller set were expressed differently,
490 and many are prime candidates for future functional analysis.
491 Multiple ABC transporters were induced by AM colonization (**Fig. 6C**), and two of these,
492 *STR* and *STR2*, have already been studied extensively (Zhang et al., 2010). Two others, *AMN2* and
493 *AMN3*, are also well studied, but their functional role remains elusive (Roy, 2015). The two
494 remaining genes, *Medtr4g124040* and *Medtr1g050525*, have not been functionally characterized
495 and could represent interesting targets for future studies. The amino acid transporters
496 *Medtr1g030660* and *Medtr2g101920* and the peptide transporters *PTR3* and *OPT15* were all
497 upregulated in mycorrhizal roots. None of these have been functionally characterized, but the
498 protein product of *Medtr2g101920* was isolated from the plasma membrane of AM roots (Aloui et

Figure 9

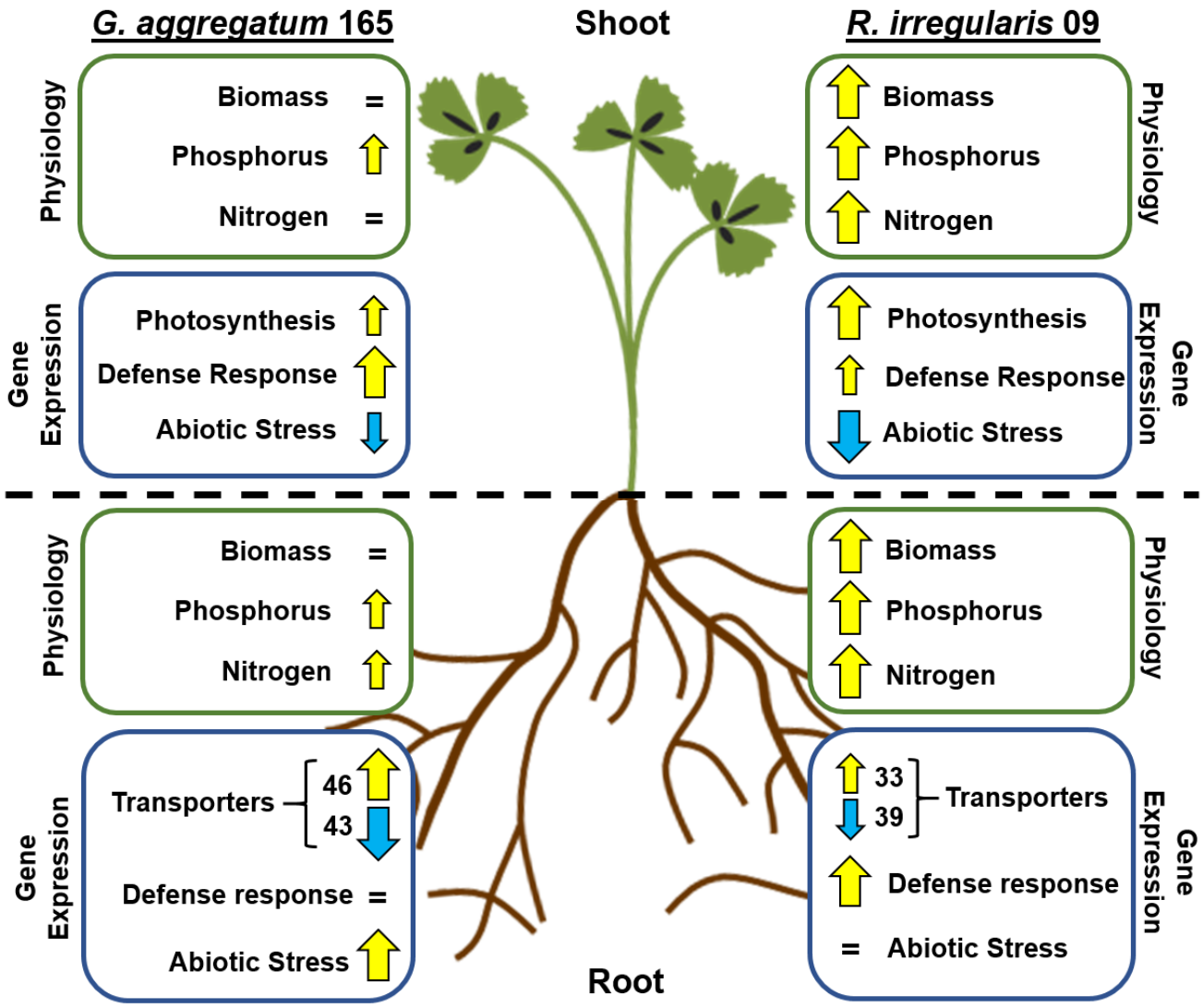

Figure 9. Summary of the physiological and transcriptomic responses in roots and shoots of *Medicago truncatula* colonized by either *Glomus aggregatum* 165 or *Rhizophagus irregularis* 09. Physiological data include the analysis of plant biomass and phosphorus and nitrogen-15 contents in plant tissues. Transcriptomic data include the expression patterns of nutrient transporters and enrichment of gene ontology terms. Yellow up-arrows indicate an increase, equal signs (=) indicate no change, and blue down-arrows indicate a decrease in each response compared to non-mycorrhizal plants. Arrow size indicates the degree of the response.

500 understanding how these mechanisms are regulated will likely allow for improved use of this
501 symbiotic association in the sustainable production of food, feed, fiber, and fuel.
502

503 **MATERIAL AND METHODS**

504 **Biological materials and growth conditions**

505 *M. truncatula* 'Jemalong A17' seeds were acid scarified in 36N H_2SO_4 (Fisher Scientific Inc.,
506 Waltham, MA, USA), surface sterilized with 8.25% sodium hypochlorite (Clorox® bleach, The
507 Clorox Company, Oakland, CA, USA), rinsed with sterile Type 1 water and imbibed at 4°C
508 overnight. The seeds were then transferred onto moist autoclaved filter paper in Petri dishes and
509 kept in the dark for 3 d. Finally, the Petri dishes were placed in ambient conditions for 7 d. Fully
510 germinated seedlings were transferred into the root compartment (RC) of a custom-made, two-
511 compartment pot measuring 12 cm x 8 cm x 8 cm (L x W x H; **Supplemental Fig. S1**). The RC
512 was separated from the hyphal compartment (HC) by a 0.1 cm-thick plastic divider sealed on all
513 sides by silicone (Aqueon, Franklin, WI, USA). A hole in the middle of the divider (~3.12 cm in
514 diameter) was covered on both sides with a sheet of fine nylon mesh with 50 µm pores. Between
515 these sheets was a coarse nylon mesh with 1000 µm pores to create an air gap and inhibit mass
516 flow between the RC and the HC. This allowed fungal hyphae, but not roots, to crossover from the
517 RC to the HC (**Supplemental Fig. S1**). Both compartments were filled with 250 ml of sterilized
518 soil substrate containing 40% sand, 20% perlite, 20% vermiculite, and 20% soil by volume. The
519 soil substrate had an original concentration of 4.81 mg kg^{-1} of Olsen's extractable phosphate, 10
520 mg kg^{-1} of NH_4^+, 34.4 mg kg^{-1} of NO_3^-, and a pH of 8.26. These nutrient levels were sufficiently
521 low to induce host demand for N and P and to stimulate AM colonization.

522 Fungal inoculum for *Rhizophagus irregularis* isolate 09 (Ri09; collected from Southwest
523 Spain by Mycovitro S.L. Biotechnología ecológica, Granada, Spain) and *Glomus aggregatum*
524 isolate 165 (Ga165; collected from the Long Term Mycorrhizal Research Site, University of
525 Guelph, Canada) were produced using axenic root organ cultures of Ri T-DNA transformed carrot
526 (*Daucus carota* clone DCI) grown on minimal medium (St-Arnaud et al., 1996). After
527 approximately eight weeks of growth, spores were isolated by blending the medium in 10 mM
528 citrate buffer (pH 6.0). Then, at transplanting, each seedling was inoculated with ~0.4 g
529 mycorrhizal roots and ~500 (long-term experiment) or ~350 (short-term experiment) spores of
530 either Ri09 or Ga165. Non-mycorrhizal (NM) controls received a similar quantity of double
531 autoclaved roots and spores. After transplanting and fungal inoculation, the plants were grown in
532 a growth chamber (model TC30; Conviron, Winnipeg, MB, Canada) with a 25°C day/20°C night
533 cycle, 30% relative humidity, and a photosynthetic photon flux of ~225 μmol m^{-2} s^{-1}.
534

535 **Experimental design**

536 Throughout the experiment, the position of the plants within the growth chamber was randomized
537 three times. In the long-term experiment, 4 mM $^{15}NH_4Cl$ (Sigma Aldrich, St. Louis, USA) and 0.5
538 mM KH_2PO4 in a modified Ingestad solution (Ingestad, 1960) were added to the HC of
539 mycorrhizal and nonmycorrhizal plants five weeks post-inoculation. The plants were harvested
540 two weeks later (seven weeks post-inoculation). For the short-term experiment, the plants were
541 harvested three weeks post-inoculation to observe arbuscular development at an earlier time point.
542

543 **Biomass determination, mycorrhizal quantification, and analysis of nitrogen and**
544 **phosphorus contents in plants**

545 At plant harvest, shoots and roots were separated to determine their respective fresh weight.
546 Aliquots of both tissues were flash frozen in liquid N_2 and stored at -80°C for transcriptome
547 analysis. An additional root aliquot was collected and stored in 50% ethanol at 4°C to assess AM
548 colonization. The remaining plant tissue was dried at 70°C for 48 h and then shoot and root dry
549 weights were recorded. To determine the level of AM colonization, root aliquots were cleared with
550 10% KOH at 80°C for 30 min, rinsed with tap water, and stained with 5% Sheaffer ink-vinegar
551 (v:v) at 80°C for 15 min (Vierheilig et al., 1998). In both experiments, total mycorrhizal
552 colonization rates were assessed using the gridline intersection method (McGonigle et al., 1990).
553 In the short-term experiment, the same staining and counting methods were used in the short-term
554 experiment, but we also specifically counted the number of arbuscules at root gridline intersections
555 where AM fungi were present. In both experiments, we did not observe any fungal structures in
556 the roots of NM control plants. Aliquots of dried shoot and root tissues were pulverized using a
557 tissue homogenizer (Precellys 24 Dual, Cayman Chemical Company, Ann Arbor, MI, USA) and
558 digested with 2N HCl for 2 h at 95°C. The P content in the plant tissues was spectrophotometrically
559 determined at 436 nm after adding ammonium molybdate vanadate solution (Fisher Scientific,
560 Pittsburgh, USA). Measurements of nitrogen-15 in plant tissues were performed by quantitative
561 NMR spectroscopy as described previously (Kafle et al., 2018).
562

563 **Fluorescent staining and confocal analysis of arbuscules**

564 Ink-stained roots from the short-term experiment that contained arbuscules were washed with
565 sterile 1X phosphate-buffered saline (PBS), incubated in 10% KOH for 2 d at room temperature,
566 neutralized in 0.1 M HCl for 3 h at room temperature, and then rinsed in sterile PBS. The roots
567 were then stained for confocal imaging as described in (Cope et al., 2019). Briefly, they were

568 incubated overnight at 4°C in PBS containing 2 µg ml^{-1} Alexa Fluor 488™ conjugated to wheat
569 germ agglutinin (WGA; Thermo Fischer Scientific, Waltham, MA, USA) and 10 µg ml^{-1}
570 propidium iodide. The next day, stained roots were mounted on a glass slide and immediately
571 observed on an Olympus FV1200 confocal laser scanning microscope (Olympus, Shinjuku,
572 Tokyo, Japan) with an Olympus UPlanApo 40×/0.85 objective. The emission spectra of Alexa
573 Fluor 488™ WGA (500 to 540 nm) and propidium iodide (580 to 630 nm) were detected after
574 excitation with 488-nm and 561-nm lasers, respectively. Other settings used in the Fluoview v4.2c
575 acquisition software (*e.g.*, laser intensity, gain, offset, magnification, airy units) were similar for
576 all sample observations.
577
578 **RNA isolation and sequencing**
579 Root and shoot tissues from four biological replicates (n = 4) were homogenized in liquid N2,
580 and total RNA was extracted using the PureLinkTM RNA Mini Kit (Thermo Fisher Scientific).
581 Extracted RNAs were treated with TURBO™ DNase (Thermo Fisher Scientific) and quantified
582 using a NanoDrop ND-2000 spectrophotometer (Thermo Fisher Scientific). RNA quality was
583 assessed using 2100 BioAnalyzer technology (Agilent Technologies). Approximately 100 ng of
584 total RNA was used to construct poly(A) selection libraries using the Illumina TruSeq RNA
585 Sample Preparation kit and 150-nucleotide single-end reads were sequenced using an Illumina
586 NextSeq500 with high output flow cells (Genomics Sequencing Facility, South Dakota State
587 University). The sequencing data were analyzed as described in the Supplemental Material and
588 Methods.
589
590 **Statistical analysis**

591 Mean and standard error of the mean were determined from five independent biological replicates
592 per treatment, unless mentioned otherwise. One-way ANOVA was used to identify statistically
593 significant differences ($p \leq 0.05$) among all three treatments for dry weight, P concentration, P
594 content, and nitrogen-15 enrichment. An LSD test was subsequently used for pairwise multiple
595 comparisons to identify significant differences ($p \leq 0.05$) among treatments. These statistical
596 analyses were conducted using Statistix 9 (analytical software, Tallahassee, FL, USA). For AM
597 colonization and arbuscule size, statistically significant differences ($p \leq 0.05$) between the Ga165
598 and Ri09 mycorrhizal treatments were determined using a two-sample t-test in R v4.0.2 (The R
599 Foundation, 2020). Only results that are significant at the $p \leq 0.05$-level are primarily discussed.
600 All F statistics and p-values are shown in **Supplemental Table S1**.
601
602 **Supplemental Data**
603 **Supplemental Figure S1.** Schematic model of the dual-compartment pot system used for this
604 study.
605 **Supplemental Figure S2**. Percent colonization of *Medicago truncatula* roots inoculated with
606 arbuscular mycorrhizal fungi.
607 **Supplemental Figure S3**. Shoot and root phosphorous concentration of Medicago truncatula
608 colonized by arbuscular mycorrhizal fungi.
609 **Supplemental Figure S4**. Hierarchical clustering of biological replicates from root RNA
610 sequencing data.
611 **Supplemental Figure S5**. Hierarchical clustering of biological replicates from shoot RNA
612 sequencing data.

613 **Supplemental Figure S6**. Volcano plots of differentially expressed genes (DEGs) between
614 treatments.
615 **Supplemental Figure S7**. Summary of gene ontology enrichment analysis of genes upregulated
616 in the roots of *Medicago trunctaula*.
617 **Supplemental Figure S8**. Summary of gene ontology enrichment analysis of genes
618 downregulated in the roots of *Medicago trunctaula*.
619 **Supplemental Figure S9**. Summary of gene ontology enrichment analysis of differentially
620 expressed genes in the shoots of *Medicago trunctaula*.
621 **Supplemental Figure S10**. Summary of arbuscular mycorrhizal colonization in *Medicago*
622 *truncatula* at three-weeks post inoculation.
623 **Supplemental Table S1.** F statistics and p-values from one-way ANOVA for each experimental
624 parameter.
625 **Supplemental Table S2**. Expression levels of genes associated with the strigolactone biosynthesis
626 pathway and the common symbiosis signaling pathway in roots of *Medicago truncatula*.
627 **Supplemental Table S3**. Expression levels of genes downstream of the common symbiosis
628 signaling pathway in roots of *Medicago truncatula*.
629 **Supplemental Table S4**. List of differentially regulated genes from shoot gene ontology
630 enrichment analysis.
631 **Supplemental Table S5**. List of differentially regulated defense response genes from root gene
632 ontology enrichment analysis.
633 **Supplemental File 1**. Significantly differentially expressed genes in roots
634 **Supplemental File 2**. Significantly differentially expressed genes in shoots
635 **Supplemental File 3**. Significant gene ontology terms in roots

636 **Supplemental File 4**. Significantly differentially expressed transporters in roots

637 **Supplemental File 5**. List of mineral transporters by type

638 **Supplemental File 6**. List of secondary metabolite transporters by type

639 **Supplemental File 7**. Significant gene ontology terms in shoots

640

641 **ACKNOWLEDGEMENTS**

642 This work was funded by the USDA (2017-67014-26530), the SD Soybean Research and
643 Promotion Council, and the Agricultural Experiment Station at SDSU to HK and SS. KG
644 acknowledges support of the North Carolina Agriculture Research Service (NCARS), the North
645 Carolina Soybean Producers Association (2019-1656), and the USDA (2020-67013-31800).

646

647 **FIGURE LEGENDS**

648 **Figure 1.** Biomass and nutrient content of *Medicago truncatula* plants colonized by different
649 arbuscular mycorrhizal fungi. Shown are dry weight (A,B), phosphorus content (C,D), and %
650 nitrogen-15 enrichment (E,F) of shoots (A,C,E) and roots (B,D,F). The plants were inoculated with
651 either *Glomus aggregatum* 165 (Ga165) or *Rhizophagus irregularis* 09 (Ri09) and compared to
652 non-mycorrhizal (NM) control plants. Bars represent the mean of each treatment ($n = 5$) ± SEM.
653 Different letters on the bars indicate statistically significant ($p \leq 0.05$) differences based on one-
654 way ANOVA and LSD test. F statistics and p-values are shown in Supplemental Table S1.

655

656 **Figure 2.** Significantly differentially expressed genes in roots (A–C) and shoots (D–F) of
657 *Medicago truncatula* colonized by different AM fungi. (A, D) Number of significantly
658 differentially expressed genes (DEGs; $\log_2$[fold-change] > 2 and a q-value < 0.05) in plants

659 colonized by *Glomus aggregatum* 165 (Ga165) or *Rhizophagus irregularis* 09 (Ri09) compared
660 either to non-mycorrhizal (NM) control plants or to each other. (B, E) Venn diagrams of
661 significantly upregulated (yellow) and downregulated (blue) DEGs unique to Ga165 and Ri09-
662 colonized plants or shared by both. (C, F) Heat maps of fragments per kilobase of transcript per
663 million mapped reads (FPKM) values + 1 for all significant DEGs from each treatment. Gene
664 clusters are assigned based on second-order branching. Upregulated genes are shown in yellow
665 and downregulated genes in blue with intensity based on row z-score. All DEGs in each plot for
666 roots and shoots are listed in Supplemental Files 1 and 2, respectively.
667
668 **Figure 3.** ***Expression patterns of genes in the strigolactone biosynthesis pathway.*** (**A**) Diagram
669 of the strigolactone biosynthesis pathway and the relative expression levels of genes in *Medicago*
670 *truncatula* that encode components of the pathway shown as fragments per kilobase of transcript
671 per million mapped reads (FPKM; blue=low, yellow=high) in roots from non-mycorrhizal (NM)
672 plants or plants colonized by either *Glomus aggregatum* 165 (Ga165) or *Rhizophagus irregularis*
673 09 (Ri09). The expression patterns (FPKM) for four specific genes upregulated by Ri09-
674 colonization are also shown, including (**B**) *More Axillary Growth 1a* (*MAX1a*), (**C**) *Carotenoid*
675 *Cleavage Dioxygenase 7* (*CCD7*), (**D**) *Nodulation Signaling Pathway 1* (*NSP1*) and (**E**) *NSP2* in
676 NM roots (n=3) and roots inoculated with Ga165 (n=3) or Ri09 (n=4). Bars represent the mean of
677 each treatment ± SEM. Significant differences (q-value < 0.05) in FPKM values between
678 treatments were determined as part of the CuffDiff2 analysis and are indicated using different
679 letters (see **Supplemental Table S2**). Abbreviations in A: GAP, glyceraldehyde 3-phosphate;
680 DXS2, 1-deoxyxylulose 5-phosphate synthase2; MEP, 2-methyl-erythritol-4-phosphate; GGDP
681 geranylgeranyl pyrophosphate; D27, Dwarf27; and PDR1a, pleiotropic drug resistance 1a.

682

683 **Figure 4.** Relative expression of six genes in the roots of *Medicago truncatula* after colonization
684 with different AM fungi. Expression of (A) *Required for Arbuscule Development 1* (*RAD1*), (B)
685 *MYB-like Transcription Factor 1* (*MYB1*), (C) *Phosphate Transporter 8* (*PT8*), (D) *Ammonium*
686 *Transporter 2;3* (*AMT2;3*), (E) *Reduced Arbuscular Mycorrhization 2* (*RAM2*), and (F) *Sugars*
687 *Will Eventually Be Exported Transporter 1.2* (*SWEET1.2*) are shown for non-mycorrhizal plants
688 (NM, n=3) and plants inoculated with *Glomus aggregatum* 165 (Ga165, n=3) or *Rhizophagus*
689 *irregularis* 09 (Ri09, n=4). Expression levels are shown as fragments per kilobase of transcript per
690 million mapped reads (FPKM). Bars represent the mean of each treatment ± SEM. Significant
691 differences (q-value < 0.05) in FPKM values between treatments were determined as part of the
692 CuffDiff2 analysis and are indicated using different letters (see Supplemental Table S3).

693

694 **Figure 5.** Expression patterns of significantly differentially expressed mineral transporter genes
695 in the roots of *Medicago truncatula* after colonization with different AM fungi. (A) Venn diagrams
696 showing the number of mineral transporters that are significantly up- (yellow) or down-regulated
697 (blue) in roots colonized by *Glomus aggregatum* 165 (Ga165) or *Rhizophagus irregularis* 09
698 (Ri09), or both. (B) Summary of the number of genes from specific gene annotation groups of
699 mineral transporters that are up- or down-regulated in roots colonized by Ga165 or Ri09, or both
700 (see also Supplemental File 5). Expression patterns of genes annotated as (C) ammonium, (D)
701 nitrate, (E) phosphate, and (F) sulfate transporters in the roots of non-mycorrhizal plants (NM)
702 (n=3) and plants inoculated with Ga165 (n=3) or Ri09 (n=4). The bars in C–F represent the mean
703 of each treatment ± SEM. Expression levels are shown as fragments per kilobase of transcript per
704 million mapped reads (FPKM), only genes with FPKM ≥ 10 are shown, significant differences (q-

705 value < 0.05) in FPKM values between treatments were determined as part of the CuffDiff2
706 analysis and are indicated using different letters on the bars.
707
708 **Figure 6.** Expression patterns of significantly differentially expressed secondary metabolite
709 transporters in the roots of *Medicago truncatula* after colonization with different AM fungi. (A)
710 Venn diagrams showing the number of secondary metabolite transporters that are significantly up-
711 (yellow) or down-regulated (blue) in roots colonized by *Glomus aggregatum* 165 (Ga165) or
712 *Rhizophagus irregularis* 09 (Ri09), or both. (B) Summary of the number of genes from specific
713 gene annotation groups of secondary metabolite transports that are up- or down-regulated in roots
714 colonized by Ga165 or Ri09, or both (see Supplemental File 6). Expression patterns of genes
715 annotated as (C) ATP-binding cassette (ABC), (D) amino acid or peptide, (E) major facilitator
716 superfamily (MFS) or major intrinsic protein (MIP), and (F) sugar transporters in the roots of non-
717 mycorrhizal plants (NM) (n = 3) and plants inoculated with Ga165 (n =3) or Ri09 (n = 4). The bars
718 in C-F represent the mean of each treatment ± SEM. Expression levels are shown as fragments per
719 kilobase of transcript per million mapped reads (FPKM); only genes with FPKM ≥ 10 are shown;
720 significant differences (q-value < 0.05) in FPKM values between treatments were determined as
721 part of the CuffDiff2 analysis and are indicated using different letters on the bars. Abbreviations
722 in B: G3P, glycerol-3-phosphate; NAT, nucleobase-ascorbate transporter; OST, organic solute
723 transporter; TPT, triose-phosphate transporter; TRAPP, transport protein particle.
724
725 **Figure 7.** Expression patterns of significantly differentially expressed genes in the shoots of
726 *Medicago truncatula* colonized by different AM fungi. Expression levels of genes involved in (A)
727 photosynthesis, (B) response to biotic stress, and (C) response to abiotic stress in non-mycorrhizal

728 plants (NM; n=4) or plants colonized by *Glomus aggregatum* 165 (Ga165, n=4) or *Rhizophagus*
729 *irregularis* 09 (Ri09, n=3). Bars represent the mean of each treatment ± SEM. Expression levels
730 are shown as fragments per kilobase of transcript per million mapped reads (FPKM), and
731 significant differences (q-value < 0.05) in FPKM values between treatments were determined as
732 part of the CuffDiff2 analysis and are indicated using different letters above the bars (see also
733 Supplemental Table S4).
734
735 **Figure 8.** Colonization patterns and arbuscule size of *Glomus aggregatum* 165 and *Rhizophagus*
736 *irregularis* 09 in *Medicago truncatula* roots three weeks post-inoculation. (A) Image of non-
737 mycorrhizal *M. truncatula* plants compared to either *G. aggregatum* 165 (Ga165) or *R. irregularis*
738 09 (Ri09) colonized plants. (B–D) Representative images of ink-stained NM roots (B), Ga165-
739 colonized roots (C), and Ri09-colonized roots (D) (scale bar = 200 µm). (E–F) Representative
740 confocal images of Ga165 (E) and Ri09-colonized (F) roots containing arbuscules and stained with
741 wheat germ agglutinin Alexafluor-488 (scale bar = 50 µm). (G) Box and whisker plots embedded
742 in violin plots displaying the size distribution for the width of all arbuscules in Ga165 (light grey)
743 and Ri09 (dark grey) colonized roots. In 11 and 15 colonized roots, 132 and 80 arbuscules were
744 evaluated for Ga165 and Ri09, respectively. The mean arbuscule width for each fungal species
745 was compared using a student's t-test (****p < 0.0001).
746
747 **Figure 9.** Summary of the physiological and transcriptomic responses in roots and shoots of
748 *Medicago truncatula* colonized by either *Glomus aggregatum* 165 or *Rhizophagus irregularis* 09.
749 Physiological data include the analysis of plant biomass and phosphorus and nitrogen-15 contents
750 in plant tissues. Transcriptomic data include the expression patterns of nutrient transporters and

751 enrichment of gene ontology terms. Yellow up-arrows indicate an increase, equal signs (=) indicate
752 no change, and blue down-arrows indicate a decrease in each response compared to non-
753 mycorrhizal plants. Arrow size indicates the degree of the response.
754

755 **LITERATURE CITED**

756 **Aloui A, Recorbet G, Lemaître-Guillier C, Mounier A, Balliau T, Zivy M, Wipf D, Dumas-**
757 **Gaudot E** (2018) The plasma membrane proteome of *Medicago truncatula* roots as
758 modified by arbuscular mycorrhizal symbiosis. Mycorrhiza **28**: 1–16

759 **Besserer A, Becard G, Jauneau A, Roux C, Sejalon-Delmas N, Bécard G, Jauneau A, Roux**
760 **C, Séjalon-Delmas N** (2008) GR24, a synthetic analog of strigolactones, stimulates the
761 mitosis and growth of the abuscular mycorrhizal fungus Gigaspora rosea by boosting its
762 energy metabolism. Plant Physiol **148**: 402–413

763 **Brundrett MC, Tedersoo L** (2018) Evolutionary history of mycorrhizal symbioses and global
764 host plant diversity. New Phytol **220**: 1108–1115

765 **Bücking H, Kafle A** (2015) Role of arbuscular mycorrhizal fungi in the nitrogen uptake of
766 plants: Current knowledge and research gaps. Agronomy **5**: 587–612

767 **Casieri L, Gallardo K, Wipf D** (2012) Transcriptional response of *Medicago truncatula*
768 sulphate transporters to arbuscular mycorrhizal symbiosis with and without sulphur stress.
769 Planta **235**: 1431–1447

770 **Chandrasekaran M** (2020) A meta-analytical approach on arbuscular mycorrhizal fungi
771 inoculation efficiency on plant growth and nutrient uptake. Agriculture **10**: 370

772 **Chen HY, Huh JH, Yu YC, Ho LH, Chen LQ, Tholl D, Frommer WB, Guo WJ** (2015) The
773 Arabidopsis vacuolar sugar transporter SWEET2 limits carbon sequestration from roots and

774 restricts *Pythium* infection. Plant J **83**: 1046–1058

775 **Cope KR, Bascaules A, Irving TBR, Venkateshwaran M, Maeda J, Garcia K, Rush TA, Ma**
776 **C, Labbé J, Jawdy S, et al** (2019) The ectomycorrhizal fungus Laccaria bicolor produces
777 lipochitooligosaccharides and uses the common symbiosis pathway to colonize Populus.
778 Plant Cell **31**: 2386–2410

779 **Doidy J, Vidal U, Lemoine R** (2019) Sugar transporters in Fabaceae, featuring SUT MST and
780 SWEET families of the model plant *Medicago truncatula* and the agricultural crop *Pisum*
781 *sativum*. PLoS One **14**: e0223173

782 **Fellbaum CR, Mensah JA, Cloos AJ, Strahan GE, Pfeffer PE, Kiers ET, Bücking H** (2014)
783 Fungal nutrient allocation in common mycorrhizal networks is regulated by the carbon
784 source strength of individual host plants. New Phytol **203**: 646–656

785 **Frare R, Ayub N, Alleva K, Soto G** (2018) The ammonium channel NOD26 is the evolutionary
786 innovation that drives the emergence, consolidation, and dissemination of nitrogen-fixing
787 symbiosis in angiosperms. J Mol Evol **86**: 554–565

788 **Garcia K, Doidy J, Zimmermann SD, Wipf D, Courty PE** (2016) Take a trip through the
789 plant and fungal transportome of mycorrhiza. Trends Plant Sci **21**: 937–950

790 **Genre A, Chabaud M, Balzergue C, Puech-Pagès V, Novero M, Rey T, Fournier J,**
791 **Rochange S, Bécard G, Bonfante P, et al** (2013) Short-chain chitin oligomers from
792 arbuscular mycorrhizal fungi trigger nuclear Ca^{2+} spiking in *Medicago truncatula* roots and
793 their production is enhanced by strigolactone. New Phytol **198**: 190–202

794 **Giovannetti M, Tolosano M, Volpe V, Kopriva S, Bonfante P** (2014) Identification and
795 functional characterization of a sulfate transporter induced by both sulfur starvation and
796 mycorrhiza formation in *Lotus japonicus*. New Phytol **204**: 609–619

797 **Grunwald U, Guo W, Fischer K, Isayenkov S, Ludwig-Müller J, Hause B, Yan X, Küster**
798 **H, Franken P** (2009) Overlapping expression patterns and differential transcript levels of
799 phosphate transporter genes in arbuscular mycorrhizal, Pi-fertilised and phytohormone-
800 treated Medicago truncatula roots. Planta **229**: 1023–1034
801 **Hart MM, Forsythe J, Oshowski B, Bücking H, Jansa J, Kiers ET** (2013) Hiding in a crowd -
802 Does diversity facilitate persistence of a low-quality fungal partner in the mycorrhizal
803 symbiosis? Symbiosis **59**: 47–56
804 **Havlin JL, Beaton JD, Tisdale SL, Nelson WL** (2014) Soil Fertility and Fertilizers: An
805 Introduction to Nutrient Management, Eighth. Pearson Education, Inc.
806 **Ingestad T** (1960) Studies on the nutrition of forest tree seedlings. III mineral nutrition of pine.
807 Physiol Plant **13**: 513–533
808 **Jansa J, Smith FA, Smith SE** (2008) Are there benefits of simultaneous root colonization by
809 different arbuscular mycorrhizal fungi? New Phytol **177**: 779–789
810 **Johnson NC, Graham JH** (2013) The continuum concept remains a useful framework for
811 studying mycorrhizal functioning. Plant Soil **363**: 411–419
812 **Kafle A, Cope KKR, Raths R, Yakha JK, Subramanian S, Bücking H, Garcia K, Krishna**
813 **Yakha J, Subramanian S, Bücking H, et al** (2019) Harnessing soil microbes to improve
814 plant phosphate efficiency in cropping systems. Agronomy **9**: 127
815 **Kafle A, Garcia K, Wang X, Pfeffer PE, Strahan GD, Bücking H** (2018) Nutrient demand
816 and fungal access to resources control the carbon allocation to the symbiotic partners in
817 tripartite interactions of *Medicago truncatula*. Plant Cell Environ 1–15
818 **Kaschuk G, Kuyper TW, Leffelaar PA, Hungria M, Giller KE** (2009) Are the rates of
819 photosynthesis stimulated by the carbon sink strength of rhizobial and arbuscular

820 mycorrhizal symbioses? Soil Biol Biochem **41**: 1233–1244

821 **Kiers ET, Duhamel M, Beesetty Y, Mensah J a, Franken O, Verbruggen E, Fellbaum CR,**
822 **Kowalchuk GA, Hart MM, Bago A, et al** (2011) Reciprocal rewards stabilize cooperation
823 in the mycorrhizal symbiosis. Science (80-) **333**: 880–882

824 **Kloppholz S, Kuhn H, Requena N** (2011) A secreted fungal effector of *Glomus intraradices*
825 promotes symbiotic biotrophy. Curr Biol **21**: 1204–1209

826 **LeBauer DS, Treseder KK** (2008) Nitrogen limitation of net primary productivity in terrestrial
827 ecosystems is globally distributed. Ecology **89**: 371–379

828 **Li Y, Duan T, Nan Z, Li Y** (2019a) Arbuscular mycorrhizal fungus alleviates alfalfa leaf spots
829 caused by *Phoma medicaginis* revealed by RNA-seq analysis. J Appl Microbiol jam.14387

830 **Li Y, Nan Z, Duan T** (2019b) *Rhizophagus intraradices* promotes alfalfa (*Medicago sativaM*)
831 defense against pea aphids (*Acyrthosiphon pisum*) revealed by RNA-Seq analysis.
832 Mycorrhiza **29**: 623–635

833 **Liu J, Maldonado-Mendoza I, Lopez-Meyer M, Cheung F, Town CD, Harrison MJ** (2007)
834 Arbuscular mycorrhizal symbiosis is accompanied by local and systemic alterations in gene
835 expression and an increase in disease resistance in the shoots. Plant J **50**: 529–544

836 **MacLean AM, Bravo A, Harrison MJ** (2017) Plant signaling and metabolic pathways enabling
837 arbuscular mycorrhizal symbiosis. Plant Cell **29**: 2319–2335

838 **Maillet F, Poinsot V, André O, Puech-Pagés V, Haouy A, Gueunier M, Cromer L, Giraudet**
839 **D, Formey D, Niebel A, et al** (2011) Fungal lipochitooligosaccharide symbiotic signals in
840 arbuscular mycorrhiza. Nature **469**: 58–64

841 **Maróti G, Downie JA, Kondorosi É** (2015) Plant cysteine-rich peptides that inhibit pathogen
842 growth and control rhizobial differentiation in legume nodules. Curr Opin Plant Biol **26**:

843 57–63

844 **Martin FM, Uroz S, Barker DG** (2017) Ancestral alliances: Plant mutualistic symbioses with
845 fungi and bacteria. Science (80-) **356**: eaad4501

846 **McGonigle TP, Miller MH, Evans DG, Fairchild GL, Swan JA** (1990) A new method which
847 gives an objective measure of colonization of roots by vesicular-arbuscular mycorrhizal
848 fungi. New Phytol **115**: 495–501

849 **Nadal M, Sawers R, Naseem S, Bassin B, Kulicke C, Sharman A, An G, An K, Ahern KR,**
850 **Romag A, et al** (2017) An N-acetylglucosamine transporter required for arbuscular
851 mycorrhizal symbioses in rice and maize. Nat Plants **3**: 1–7

852 **Pimprikar P, Gutjahr C** (2018) Transcriptional Regulation of Arbuscular Mycorrhiza
853 Development. Plant Cell Physiol **59**: 673–690

854 **Postnikova OA, Shao J, Nemchinov LG** (2013) Analysis of the alfalfa root transcriptome in
855 response to salinity stress. Plant Cell Physiol **54**: 1041–1055

856 **Roth R, Paszkowski U** (2017) Plant carbon nourishment of arbuscular mycorrhizal fungi. Curr
857 Opin Plant Biol **39**: 50–56

858 **Roux SJ, Clark GB, Morgan RO, Fernandez M-PP, Roux SJ** (2012) Evolutionary adaptation
859 of plant annexins has diversified their molecular structures, interactions and functional
860 roles. New Phytol **196**: 695–712

861 **Roy S** (2015) Analysis of gene expression, regulation, and function of three symbiotic ABC
862 subfamily-B transporters in *Medicago truncatula*.

863 **Rush TA, Puech-Pagès V, Bascaules A, Jargeat P, Maillet F, Haouy A, Maës AQM, Carriel**
864 **CC, Khokhani D, Keller-Pearson M, et al** (2020) Lipo-chitooligosaccharides as
865 regulatory signals of fungal growth and development. Nat Commun **11**: 1–10

866 **Sameeullah M, Demiral T, Aslam N, Baloch FS, Gurel E** (2016) In silico functional analyses
867 of SWEETs reveal cues for their role in AMF symbiosis. Plant, Soil Microbes Vol. 2 Mech.
868 Mol. Interact. Springer International Publishing, pp 45–58
869 **Sharma E, Anand G, Kapoor R** (2017) Terpenoids in plant and arbuscular mycorrhiza-
870 reinforced defence against herbivorous insects. Ann Bot **119**: 791–801
871 **Sieh D, Watanabe M, Devers EA, Brueckner F, Hoefgen R, Krajinski F** (2013) The
872 arbuscular mycorrhizal symbiosis influences sulfur starvation responses of Medicago
873 truncatula. New Phytol **197**: 606–616
874 **Spatafora JW, Chang Y, Benny GL, Lazarus K, Smith ME, Berbee ML, Bonito G, Corradi**
875 **N, Grigoriev I, Gryganskyi A, et al** (2016) A phylum-level phylogenetic classification of
876 zygomycete fungi based on genome-scale data. Mycologia **108**: 1028–1046
877 **St-Arnaud M, Hamel C, Vimard B, Caron M, Fortin JA** (1996) Enhanced hyphal growth and
878 spore production of the arbuscular mycorrhizal fungus Glomus intraradices in an in vitro
879 system in the absence of host roots. Mycol Res **100**: 328–332
880 **Tang H, Krishnakumar V, Bidwell S, Rosen B, Chan A, Zhou S, Gentzbittel L, Childs KL,**
881 **Yandell M, Gundlach H, et al** (2014) An improved genome release (version Mt4.0) for the
882 model legume Medicago truncatula. BMC Genomics **15**: 312
883 **Tejada-Jiménez M, Gil-Díez P, León-Mediavilla J, Wen J, Mysore KS, Imperial J,**
884 **González-Guerrero M** (2017) Medicago truncatula Molybdate Transporter type 1
885 (MtMOT1.3) is a plasma membrane molybdenum transporter required for nitrogenase
886 activity in root nodules under molybdenum deficiency. New Phytol **216**: 1223–1235
887 **Uhe M, Hogekamp C, Hartmann RM, Hohnjec N, Küster H** (2018) The mycorrhiza-
888 dependent defensin MtDefMd1 of Medicago truncatula acts during the late restructuring

889 stages of arbusculecontaining cells. PLoS One **13**: e0191841

890 **Vierheilig H, Coughlan AP, Wyss U, Piché Y** (1998) Ink and vinegar, a simple staining
891 technique for arbuscular-mycorrhizal fungi. Appl Environ Microbiol **64**: 5004–5007

892 **Vitousek PM, Porder S, Houlton BZ, Chadwick OA** (2010) Terrestrial phosphorus limitation:
893 mechanisms, implications, and nitrogen–phosphorus interactions. Ecol Appl **20**: 5–15

894 **Wang S, Chen A, Xie K, Yang X, Luo Z, Chen J, Zeng D, Ren Y, Yang C, Wang L, et al**
895 (2020) Functional analysis of the OsNPF4.5 nitrate transporter reveals a conserved
896 mycorrhizal pathway of nitrogen acquisition in plants. Proc Natl Acad Sci U S A. doi:
897 10.1073/pnas.2000926117

898 **Wang T, Zhao M, Zhang X, Liu M, Yang C, Chen Y, Chen R, Wen J, Mysore KS, Zhang**
899 **WH** (2017) Novel phosphate deficiency-responsive long non-coding RNAs in the legume
900 model plant Medicago truncatula. J Exp Bot **68**: 5937–5948

901 **Wang X, Zhao S, Bücking H** (2016) Arbuscular mycorrhizal growth responses are fungal
902 specific but do not differ between soybean genotypes with different phosphate efficiency.
903 Ann Bot **118**: 11–21

904 **Wipf D, Mongelard G, van Tuinen D, Gutierrez L, Casieri L** (2014) Transcriptional
905 responses of Medicago truncatula upon sulfur deficiency stress and arbuscular mycorrhizal
906 symbiosis. Front Plant Sci **5**: 680

907 **Wright DP, Read DJ, Scholes JD** (1998) Mycorrhizal sink strength influences whole plant
908 carbon balance of Trifolium repens L. Plant, Cell Environ **21**: 881–891

909 **Yoneyama K, Yoneyama K, Takeuchi Y, Sekimoto H** (2007) Phosphorus deficiency in red
910 clover promotes exudation of orobanchol, the signal for mycorrhizal symbionts and
911 germination stimulant for root parasites. Planta **225**: 1031–1038

912 **Zhang YM, Wang HQ, Liu DM, Liu RJ** (2020) Three tandemly aligned lea genes from
913 medicago truncatula confer differential protection to Escherichia coli against abiotic
914 stresses. Biol Plant **64**: 95–103
915